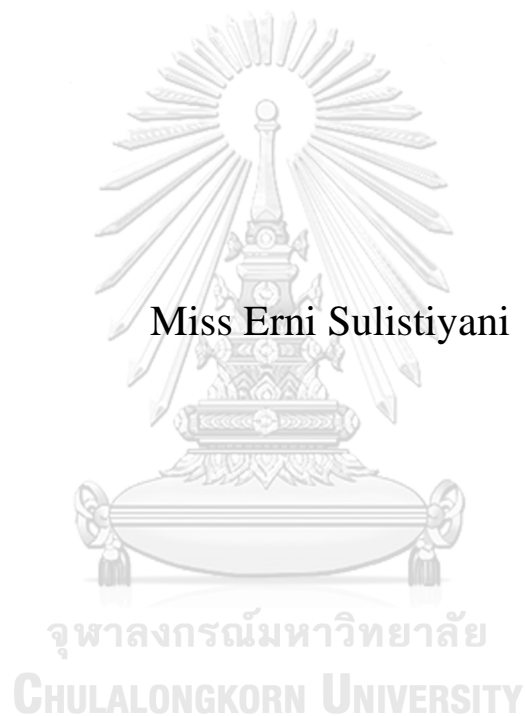


**BIOLOGICAL EFFECTS OF EPIGALLOCATECHIN
GALLATE DURING THE PROTECTION OF THE
SUBMANDIBULAR GLAND AFTER INJURY**



A Thesis Submitted in Partial Fulfillment of the Requirements
for the Degree of Master of Science in Oral Biology
Common Course
FACULTY OF DENTISTRY
Chulalongkorn University
Academic Year 2020
Copyright of Chulalongkorn University

ผลทางชีวภาพของอีพิกัลโลคาเทชินกัลเลตต่อการป้องกันต่อม้ามน้ำลายใต้ขากรรไกรจากการได้รับ
บาดเจ็บ



วิทยานิพนธ์นี้เป็นส่วนหนึ่งของการศึกษาตามหลักสูตรปริญญาวิทยาศาสตรมหาบัณฑิต
สาขาวิชาชีววิทยาช่องปาก ไม่สังกัดภาควิชา/เทียบเท่า
คณะทันตแพทยศาสตร์ จุฬาลงกรณ์มหาวิทยาลัย
ปีการศึกษา 2563
ลิขสิทธิ์ของจุฬาลงกรณ์มหาวิทยาลัย

เออร์นี สุทธิสอียานี : ผลทางชีวภาพของอีพิแกลโลคาเทชินกัลเลตต่อการป้องกันต่อมน้ำลายใต้ขากรรไกรจากการได้รับบาดเจ็บ . (**BIOLOGICAL EFFECTS OF EPIGALLOCATECHIN GALLATE DURING THE PROTECTION OF THE SUBMANDIBULAR GLAND AFTER INJURY**) อ.ที่ปรึกษาหลัก :
 ผศ.ทพ. ดร.โจวแอล นูนู แอนคร้าครี วิริชชะ พีเรียชะ

ความเป็นมา: การได้รับรังสีเพื่อรักษาผู้ป่วยมะเร็งบริเวณศีรษะและลำคอในแต่ละครั้งนั้น ส่งผลให้เซลล์เอพิเธลิอิมชนิดที่สร้างสารคัดหลั่งของต่อมน้ำลายเกิดการบาดเจ็บชนิดที่ไม่กลับคืนสู่ภาวะปกติมากกว่าร้อยละ 60 ซึ่งนำไปสู่การเกิดภาวะปากแห้งหรือซีโรสโตเมีย ในการใช้รังสีรักษาเพื่อยับยั้งการเจริญของเซลล์มะเร็งบริเวณศีรษะและลำคอนั้นจะทำให้มีการเพิ่มขึ้นของอนุมูลอิสระที่ก่อให้เกิดการบาดเจ็บในหน่วยพันธุกรรมของเซลล์ในเนื้อเยื่อและอวัยวะใกล้เคียง เช่น ต่อมน้ำลาย สารอีพิแกลโลคาเทชินกัลเลต เป็นสารสำคัญในกลุ่มโพลีฟีนอลที่พบได้ในชาเขียวและมีฤทธิ์ต้านอนุมูลอิสระ ทั้งนี้เคยมีการศึกษาภายในหลอดทดลองด้วยเซลล์ไลน์เพาะเลี้ยงจากต่อมน้ำลาย พบว่าสารอีพิแกลโลคาเทชินกัลเลตสามารถปกป้องเซลล์ต่อมน้ำลายจากรังสีแกมมาได้ แต่อย่างไรก็ตามในการศึกษาถึงประสิทธิภาพของสารอีพิแกลโลคาเทชินกัลเลตในการคงสมดุลภายในเซลล์เอพิเธลิอิมของต่อมน้ำลายนั้นยังไม่มีความเข้าใจอย่างชัดเจนมากนัก จึงมีความจำเป็นในการศึกษาต่ออีกครั้งนี้

วัตถุประสงค์: เพื่อศึกษาฤทธิ์ของสารอีพิแกลโลคาเทชินกัลเลตต่อกระบวนการคงสภาวะสมดุลของเซลล์เอพิเธลิอิมในต่อมน้ำลาย และทดสอบฤทธิ์ของสารอีพิแกลโลคาเทชินกัลเลตต่อการปกป้องต่อมน้ำลายจากการบาดเจ็บที่เกิดจากการกระตุ้นด้วยกระบวนการรังสีรักษา

วิธีการศึกษา: ในกลุ่มตัวอย่างของต่อมน้ำลายที่สภาวะสมดุลนั้น ได้ทำการเพาะเลี้ยงต่อมน้ำลายชั้นเมดิบิวลาร์ที่แยกได้จากตัวอ่อนของหนูเมาส์ด้วยสารอีพิแกลโลคาเทชินกัลเลตที่ความเข้มข้น 7.5-30 ไมโครกรัมต่อมิลลิลิตร เป็นเวลา 72 ชั่วโมง จากนั้นตรวจวัดการแตกแขนงของเซลล์เอพิเธลิอิมโดยการตรวจด้วยวิธีทางกล้องจุลทรรศน์ การย้อมพิเศษทางอิมมูโนฮิสโตเคมี และการตรวจวัดการแสดงออกของยีน โดยเทคนิคอาร์เรย์ สำหรับกลุ่มตัวอย่างต่อมน้ำลายที่มีการบาดเจ็บนั้น ได้ทำการทดสอบด้วยรังสีจากเครื่องเร่งอนุภาคเชิงเส้นในช่วงปริมาณ 5-10 เกรย์ เพื่อหาปริมาณรังสีที่เหมาะสมต่อการกระตุ้นให้เกิดการบาดเจ็บจากการใช้รังสีรักษา ทั้งนี้ได้ทำการทดสอบต่อมน้ำลายด้วยสารอีพิแกลโลคาเทชินกัลเลตที่ความเข้มข้น 7.5-15 ไมโครกรัมต่อมิลลิลิตรเป็นเวลา 24 ชั่วโมง ก่อนนำไปฉายรังสีที่ปริมาณ 7 เกรย์ เพื่อเปรียบเทียบผลที่ได้กับกลุ่มที่ไม่ได้รับการฉายรังสีและกลุ่มควบคุมผลบวกภายหลังการเพาะเลี้ยงเป็นเวลา 48 ชั่วโมง ด้วยการตรวจนับการเจริญของปุ่มเซลล์เอพิเธลิอิมโดยวิธีทางกล้องจุลทรรศน์ในทุกๆ 24 ชั่วโมง ทั้งนี้ยังได้ทำการตรวจโดยวิธีทางกล้องจุลทรรศน์แบบคอนโฟคอล ชนิดที่ไซ้เลเซอร์ในการสแกน การแสดงออกของยีนโดยเทคนิคอาร์เรย์ การตรวจหาภาวะเครียดออกซิเดชัน และการย้อมพิเศษทางอิมมูโนฮิสโตเคมีแบบโพลีมาต์

ผลการศึกษา: ในกลุ่มตัวอย่างต่อมน้ำลายเพาะเลี้ยง พบว่าสารอีพิแกลโลคาเทชินกัลเลตที่ความเข้มข้น 7.5 ไมโครกรัมต่อมิลลิลิตรสามารถคงสภาวะสมดุลของเซลล์เอพิเธลิอิมของต่อมน้ำลายได้ในระหว่างกระบวนการพัฒนา และเมื่อกระตุ้นให้เกิดการบาดเจ็บด้วยการฉายรังสี พบว่ากลุ่มที่ผ่านทดสอบด้วยสารอีพิแกลโลคาเทชินกัลเลตที่ความเข้มข้น 7.5 ไมโครกรัมต่อมิลลิลิตรมาก่อน สามารถป้องกันกระบวนการเติบโต การแบ่งตัวแบบไมโทซิส และการเจริญของเซลล์เอพิเธลิอิม ทำให้มีการพัฒนาของเซลล์เอพิเธลิอิมในส่วนของอะซินาและส่วนของท่อภายในต่อมน้ำลายได้อย่างสมบูรณ์ สามารถเพิ่มจำนวนของเซลล์ต้นกำเนิดชนิด SOX2⁺ ลดจำนวนเซลล์ที่ตายแบบอะพอโทซิสจากการกระตุ้นด้วยรังสี และสามารถลดระดับของโปรตีนบ่งชี้สภาวะเครียดออกซิเดชันได้

ประโยชน์ที่ได้รับ: งานวิจัยนี้จะส่งผลให้เกิดความรู้และความเข้าใจในฤทธิ์ของสารอีพิแกลโลคาเทชินกัลเลตต่อการปกป้องต่อมน้ำลายจากการบาดเจ็บที่เกิดจากการกระตุ้นด้วยการฉายรังสี

สาขาวิชา ชีววิทยาช่องปาก
 ปีการศึกษา 2563

ลายมือชื่อนิสิต
 ลายมือชื่อ อ.ที่ปรึกษาหลัก

6175855432 : MAJOR ORAL BIOLOGY

KEYWORD: salivary gland, submandibular gland, radiotherapy, dry mouth, xerostomia

Erni Sulistiyani : BIOLOGICAL EFFECTS OF EPIGALLOCATECHIN GALLATE DURING THE PROTECTION OF THE SUBMANDIBULAR GLAND AFTER INJURY . Advisor: Asst. Prof. JOAO NUNO ANDRADE REQUICHA FERREIRA, D.D.S., M.Sc., Ph.D

Background: When radiotherapy is delivered to head and neck cancer (HNC) patients, the salivary gland (SG) secretory epithelia can be irreversibly injured in up to 60% of the individuals, leading to dry mouth or xerostomia. Radiotherapy's effectiveness in suppressing HNC growth is correlated with an increase in free radicals that produce DNA damage to the tumor and neighboring organs like the SG. Epigallocatechin gallate (EGCG) is one of the most abundant polyphenols present in green tea leaves and a well-known antioxidant. In previous *in vitro* study using genetically modified immortal SG cell lines, EGCG protected SG cells from γ -radiation. However, the ability of EGCG to maintain SG epithelia during homeostasis and to provide radioprotection for SG organ is poorly understood, and thus it requires further investigations.

Aim: To investigate whether EGCG supports epithelial maintenance during salivary gland homeostasis and determine if EGCG protects the salivary gland from epithelial injury induced by radiotherapy.

Methods: In the homeostasis SG developmental model, *ex vivo* fetal mouse submandibular glands were cultured with EGCG for 72h at 7.5-30 $\mu\text{g/mL}$. Next, SG epithelial branching morphogenesis was measured by bright-field microscopy and gene expression arrays. In the injury SG model, conventional linear accelerator (LINAC) technology for radiotherapy was used at 5-10 Gy to determine the optimal dose for generating radiation injury. To confer EGCG protection, glands were pretreated with EGCG at 7.5-15 $\mu\text{g/mL}$ for 24 hours and induced by 7 Gy and then compared to the irradiated group after cultured for 48h. To measure the end bud growth, epithelial growth quantification using bright-field microscopy was performed every 24h. Laser confocal scanning microscopy, gene expression arrays, the Griess assay, and whole-mount immunohistochemistry (IHC) were used to evaluate the biological effects of EGCG on SG epithelial cells.

Results: In *ex vivo* SG organ culture conditions, EGCG at 7.5 $\mu\text{g/mL}$ maintained epithelial SG homeostasis during development. After radiation injury, EGCG pre-treatment protected the growth, mitosis, and maturation of the epithelia, generated a mature SG epithelial acinar and ductal compartment, increased the epithelial stem cell niche (Sox2⁺), decreased radiation-induced cellular apoptosis, and reduced the oxidant stress markers.

Benefit: This research work led to a better understanding of the therapeutic potential of EGCG to prevent radiation-induced epithelial SG injury in the *ex vivo* fetal organ.

จุฬาลงกรณ์มหาวิทยาลัย
CHULALONGKORN UNIVERSITY

Field of Study: Oral Biology
Academic Year: 2020

Student's Signature
Advisor's Signature

ACKNOWLEDGEMENTS

All praise be to Allah, who bestows every blessing and strength necessary to complete my thesis.

The completion of this study could not have been possible without the expertise of Asst. Prof. Joao Nuno Andrade Requicha Ferreira, D.D.S., M.Sc., Ph.D, my advisor. I am deeply grateful to him for his guidance during each stage of my master's educational period.

I would also like to thank my committees; Prof. Prasit Pavasant, D.D.S., Ph.D, Nuttha Klincumhom, D.V.M., Ph.D, and Asst. Prof. Sasitorn Rungarunlert, D.V.M., Ph.D, for valuable comments and suggestions to improve my thesis.

I would like to acknowledge my gratitude for the opportunity to study in the Faculty of Dentistry, Chulalongkorn University, which was supported by ASEAN Scholarship 48, and the grant for this research was provided by the 90th Anniversary of Chulalongkorn University Scholarship, Ratchadapisek Somphot Fund 2563 from Graduate School and Faculty Research Grant, Faculty of Dentistry, Chulalongkorn University.

I want to express my sincere gratitude to all teachers and staff for their knowledge and support all the time. Many thanks to my colleagues at Oral Biology Master and Doctoral Program and my colleagues in 3D BioprintMe Lab for their kind help and friendly atmosphere.

Lastly, my appreciation goes to my family and friends for their encouragement, support, and love all through my studies.

Erni Sulistiyani

TABLE OF CONTENTS

	Page
.....	iii
ABSTRACT (THAI)	iii
.....	iv
ABSTRACT (ENGLISH).....	iv
ACKNOWLEDGEMENTS	v
TABLE OF CONTENTS.....	vi
List of Figures	1
List of Tables	3
List of Abbreviation.....	4
1. Introduction.....	7
1.1 Background and Rationale.....	7
1.2 Research Questions.....	8
1.3 Research Objectives.....	8
1.4 Research Hypothesis.....	9
1.6 Conceptual framework.....	9
2. Literature Review.....	10
2.1 Salivary Gland Development and Physiology.....	10
2.2 Ionizing Radiation Principles	14
2.3 Radiotherapy for HNC	15
2.4 Current therapies to prevent radiotherapy damage -Amifostine.....	18
2.5. Epigallocatechin gallate.....	21
3. Material and Methods	25
3.1 Salivary gland <i>ex vivo</i> culture.....	25
3.2 Quantification of SMG Epithelial Growth	27
3.3 Quantitative real-time polymerase chain reaction	27

3.4 Whole mount immunohistochemistry.....	28
3.5 Transmission electron microscopy	30
3.6 Griess Assay	31
3.6 Data analysis.....	31
4. Results.....	32
4.1 Objective 1: Identify whether EGCG supports epithelial maintenance during salivary gland homeostasis.	32
4.1.1 Effect of EGCG on developing SG epithelial growth.....	32
4.1.2 Biological effects of EGCG on the expression of SG specific genes	34
4.2 Objective 2: Determine whether EGCG protects the salivary gland from epithelial injury induced by radiotherapy.....	36
4.2.1 Radiotherapy generated epithelial injury on developing SG.....	36
4.2.2 EGCG protected SMG epithelial growth from radiation injury.....	37
4.2.4 EGCG protected SMG progenitor cells from radiation injury	40
4.2.5 EGCG prevented SMG cell from apoptosis induced by radiotherapy	44
5. Discussion and Conclusion.....	48
Appendix Figure 1.	53
REFERENCES	55
VITA.....	64

List of Figures

Figure 2.1.	Schematic diagram of the adult salivary gland secretory unit	Page 10
Figure 2.2.	Location of major salivary glands in humans and mouse	Page 11
Figure 2.3.	Stages of salivary gland development	Page 13
Figure 2.4.	ROS and DNA binding	Page 18
Figure 2.5.	Structure of amifostine.....	Page 19
Figure 2.6.	Structure of pilocarpine.....	Page 20
Figure 2.7.	Structure of epigallocatechin gallate (EGCG)	Page 22
Figure 3.1.	Methodology for the SG homeostasis and radiation injury models.....	Page 25
Figure 4.1.	Effect of EGCG on developing SMG epithelial growth.....	Page 32
Figure 4.2.	Effect of EGCG on gene expression in the SG with EGCG treatment	Page 34
Figure 4.3.	Effect of LINAC radiation exposure on SG epithelial injury	Page 36
Figure 4.4.	Effect of EGCG on protecting SMG epithelial growth from radiation injury.....	Page 38
Figure 4.5.	Expression of epithelial proliferation and SG epithelial markers with EGCG pre-treatment after IR injury	Page 40
Figure 4.6.	Heatmap expression of other stem/progenitors and SG differentiated markers with EGCG pre-treatment after IR injury	Page 42
Figure 4.7.	Expression of pro-apoptotic Caspase 3 marker in EGCG pre-treated glands after IR injury.	Page 45

Figure 4.8. Transmission electron micrographs of SG with EGCG pre-treatment after IR injury.....Page 45



List of Tables

Table 1.	List of oligonucleotide primer sequences.....	Page 27
Table 2.	List of primary and secondary antibodies.....	Page 29



List of Abbreviation

Abbreviation	Definition
AKT	Ak Strain Transforming
ANOVA	Analysis of variance
AQP5	Aquaporin 5
ASEAN	Association of Southeast Asian Nations
AU	Arbitrary Units
BSA	Bovine Serum Albumin
CASP3	Caspase 3
CD31	Cluster of Differentiation 31
CO ₂	Carbon Dioxide
CT	Cycle Threshold
CTL	Control
CU	Chulalongkorn University
DMEM	Dulbecco's Modified Eagle Medium
DNA	Deoxyribonucleic Acid
EGCG	Epigallocatechin-3-Gallate
ERK	Extracellular Signal-Regulated Kinase
FDA	Food and Drug Administration
FGFR2	Fibroblast Growth Factor Receptor 2
GM	Growth Medium
H	Hours
H ₂ O ₂	Hydrogen Peroxide
H ₂ AX	H2A Histone Family Member X
H ₂ O	Dihydrogen Monoxide
HNC	Head and Neck Cancer
HO*	Hydroxyl Radical
HO ₂	Heme Oxygenase-2
IACUC	Institutional Animal Care and Use Committee
IBC	Institutional Biosafety Committee

ICR	Institute of Cancer Research
IHC	Immunohistochemistry
IMRT	Intensity-Modulated Radiation Therapy
IR	Ionizing Radiation
JEOL	Japan Electron Optics Laboratory
KIT	Receptor Tyrosine Kinase Type III
KRT14	Cytokeratin 14
KRT19	Cytokeratin 19
KRT5	Cytokeratin 5
LINAC	Linear Accelerator
LSM	Laser Scanning Microscopy
M1	Muscarinic receptor 1
M3	Muscarinic receptor 3
MAPK	Mitogen-Activated Protein Kinase
MDM2	Murine Double Minute 2
MIST1	Class A basic helix-loop-helix protein 15
MOM	Mouse on Mouse
MV	Mega-Electron-Volt
NED	N-1-naphthylethylenediamine dihydrochloride
NFE2	Nuclear Factor Erythroid 2
NO ₂	Nitrogen Dioxide
O ₂	Oxygen
O ₃	Ozone
OH	Hydroxyl
PBS	Phosphate-Buffered Saline
PCR	Polymerase Chain Reaction
PG	Parotid Gland
PI3K	Phosphoinositide 3-Kinase
PRDX6	Peroxiredoxin 6

PUMA	p53 Upregulated Modulator of Apoptosis
RNA	Ribonucleic Acid
ROI	Region of Interest
ROS	Reactive Oxygen Species
RT	Radiation Therapy
SEM	Standard Error Mean
SG	Salivary Gland
SLG	Sublingual Gland
SMA	Smooth Muscle Actin
SMG	Submandibular Gland
SOX	Sex-Determining Region Y box
SOX10	Sex Determining Region Y box 10
SOX2	Sex-Determining Region Y box 2
SOX9	Sex-Determining Region Y box 9
SRY	Sex-Determining Region Y
TUBB3	Class III β -tubulin
UV	Ultraviolet
VEGFR2	Vascular Endothelial Growth Factor Receptor-2
WHO	World Health Organization
ZEN	ZEISS Efficient Navigation



1. Introduction

1.1 Background and Rationale

Based on WHO 2020 database [1], the estimated prevalence of head and neck cancers (HNC) was 12% globally, and in Thailand, it was 13%. This cancer type sat in the top ten most common cancers in Thailand [2].

To attenuate cancer progression, approximately 50% of cancer patients undergo radiotherapy [3], either single or combined with adjuvant chemotherapy [4]. Currently, radiotherapy approaches such as Intensity-Modulated Radiation Therapy [5] use a linear accelerator to deliver high-energy X-ray photon radiation. Energy from X-rays will cause cell damage by disrupting the DNA [6]. However, DNA damage is generated not only in the tumor cells but also in normal neighboring or non-targeting cells [7, 8]. The salivary glands (SG) location is often within the radiation field as HNC expands to lymphatic chains in close proximity to the glands [9]. Salivary glands are sensitive to radiotherapy and chemotherapy, thus they are subject to injury during cancer treatment [10, 11]. According to a systematic review on SG hypofunction after radiotherapy for HNC, such therapy substantially reduces the salivary flow rate, and 40-60% end up with xerostomia [12]. Submandibular glands, one of the major salivary glands, produce 65-70% of the whole saliva at rest [13]. When the radiotherapy hits submandibular glands, these glands will get injury and may result in salivary gland hypofunction due to epithelial damage in the secretory units [14].

To date, there is only one cytoprotective drug named amifostine that can be utilized to prevent radiotherapy-induced toxicity to SG epithelial cells in HNC patients [15]. This drug increases salivation and decreases xerostomia severity in up

to 27% of HNC cases [16, 17]. After amifostine is administered (15-30 minutes before radiotherapy) [18, 19], at least 53% of cancer patients suffer from severe drug side effects [16]. Such side effects include nausea, vomiting [16], and hypotension [18]. Often, these side effects lead to termination of the drug and radiotherapy delay in up to 25% of the patients [20].

Epigallocatechin gallate or EGCG is a well-known antioxidant and cytoprotective agent present in green tea leaves (*Camellia sinensis*) with unreported side effects [21]. EGCG can protect immortalized epithelial SG cell cultures *in vitro* from gamma ionizing radiation injury by inhibition of p21 and p53 in an independent manner [22]. However, the ability of EGCG to maintain SG epithelia during homeostasis and provide radioprotection after damage induced by high energy photon radiation are not well understood. Therefore, this knowledge deficit made us formulate the following questions and objectives below:

1.2 Research Questions

1. What are the EGCG-mediated biological mechanisms that support epithelial maintenance during salivary gland homeostasis?
2. What are the EGCG-mediated biological mechanism that protects the salivary gland from epithelial injury induced by radiotherapy?

1.3 Research Objectives

1. Identify whether EGCG supports epithelial maintenance during salivary gland homeostasis.
2. Determine whether EGCG protects the salivary gland from epithelial injury induced by radiotherapy.

1.4 Research Hypothesis

H_{a1}: Epigallocatechin gallate can support epithelial growth in the salivary gland during regular development and homeostasis.

H₀₁: Epigallocatechin gallate cannot support epithelial growth in the salivary gland during regular development and homeostasis.

H_{a2}: Epigallocatechin gallate can protect against oxidative stress-induced epithelial salivary gland injury.

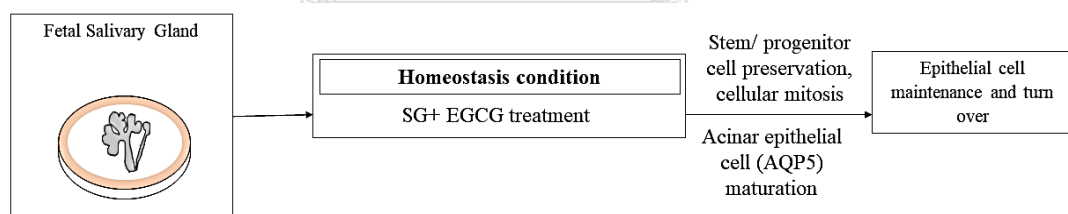
H₀₂: Epigallocatechin gallate cannot protect against oxidative stress-induced salivary gland injury.

1.5 Research design

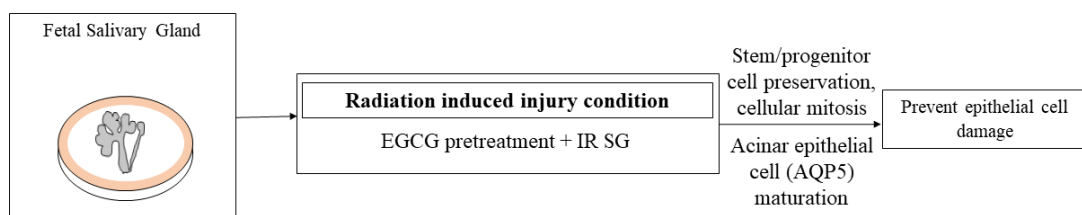
Ex vivo experimental study

1.6 Conceptual framework

Objective #1:



Objective #2:



2. Literature Review

2.1 Salivary Gland Development and Physiology

In the oral cavity, saliva is a fluid generated by exocrine glandular organs named the salivary glands [23]. The salivary gland is composed of several secretory units that produce saliva, and each secretory unit has its secretory end buds surrounded by myoepithelial and branched ductal systems. The secretory end bud consist of acinar cells are called acini [24]. Acinar cells can be serous cells or mucous cells [25], depending on the type of secretion. Serous if the cells produce watery secretion and mucous when the cells generate viscous secretion. The secretion from the end buds is named primary saliva and it will pass through along the duct and changes its compositions, then the saliva is secreted to the oral cavity [26].

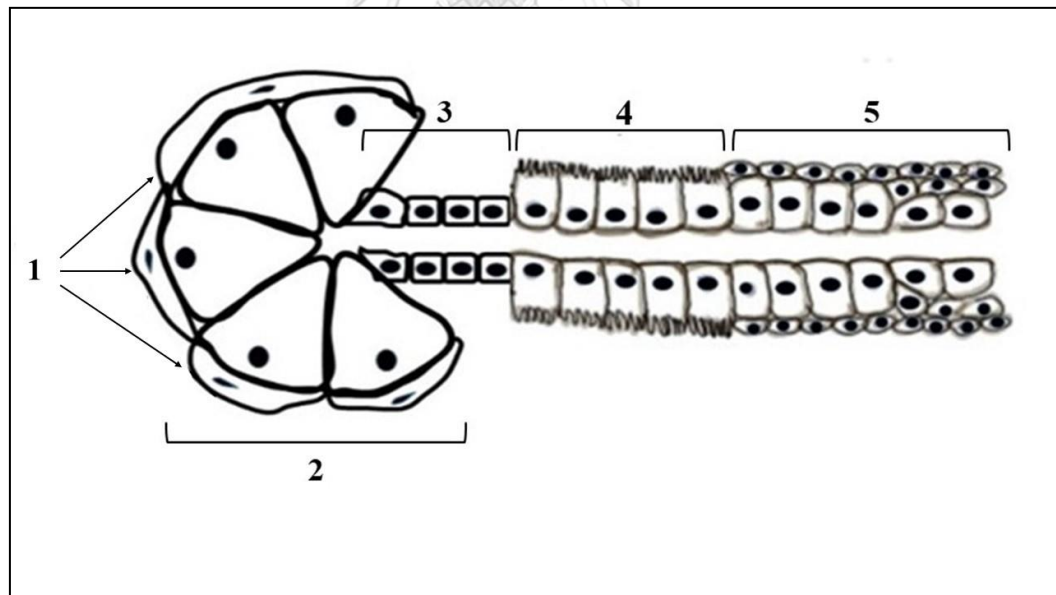


Figure 2.1. Schematic diagram of the adult salivary gland secretory unit epithelial secretory unit. 1-Myoepithelial cells; 2- Epithelial Acinar cells; 3-Epithelial Intercalated duct cells; 4-Epithelial Striated duct cells; 5-Epithelial Excretory duct cells

Both in humans and murine, there are three pairs of major salivary glands, which are the parotid glands (PG), submandibular gland (SMG), and sublingual gland (SLG) [26]. The minor salivary glands are smaller exocrine organs spreading all over the oral mucous [27].

Saliva acts to wet, lubricate, and protect oral mucous, buffering action, remineralization, antibacterial action, and supports digestion [28]. If one of these functions is disrupted, the balance within the oral cavity is affected as well.

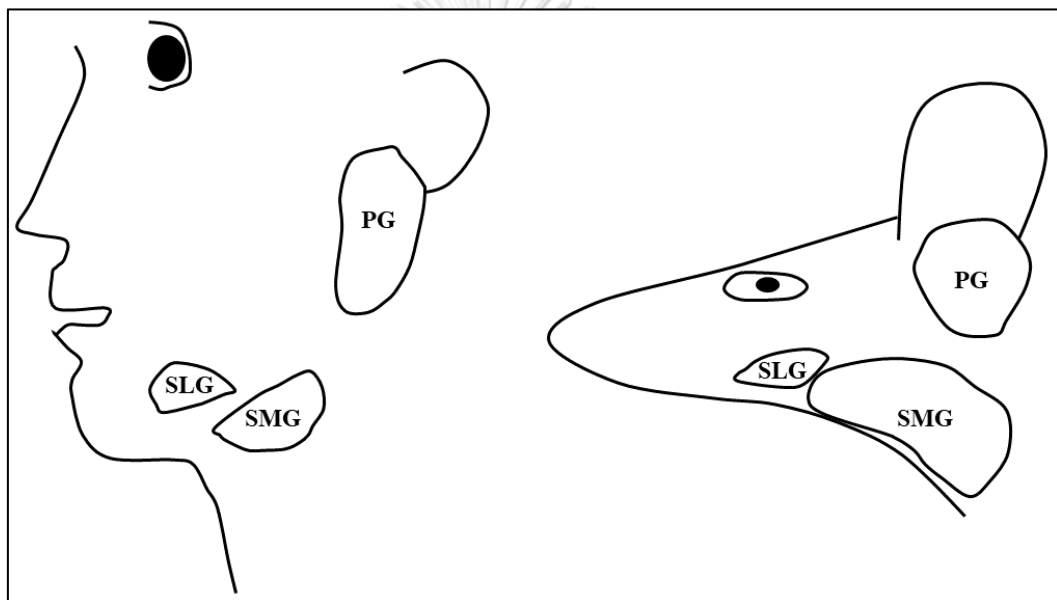


Figure 2.2. Location of major salivary glands in humans and mouse. Legend: PG, parotid gland; SLG, sublingual gland; SMG, submandibular gland

Our understanding of salivary gland development is based on the research mainly done on the SMG of rodents. At embryonic day 11.5 (E11.5), a thickening of the oral epithelium occurred next to the base of the tongue, known as placode [29, 30], and this stage is named as pre-bud stage [31].

At E12, the thickening of the oral epithelium begins larger and penetrates the mesenchyme and condenses along the epithelium [31, 32]. A single bud/primary bud/initial bud is formed at this time point and it comprises SRY-box transcription factor (SOX) SOX2⁺, SOX10⁺, and SOX9⁺ cells [33, 34]. As the epithelial bud enlarges, clefts develop at E12.5 [30, 35] and initiate the branching morphogenesis. By E13, in harmony with the enlargement of the end buds, the clefting process generates 3-5 end buds which contain KIT⁺ cells [36] and secondary duct form by branching morphogenesis [37].

At E13.5, at the pseudo glandular stage, the structure of SG can be separated into the distal and proximal epithelial region [33] and the differentiation of the SG is starting. The gland starts becoming multi-lobular. The duct begins to enlarge, and more mature progenitors are now cytokeratin 19 (KRT19) positive [38].

Meanwhile, the parasympathetic submandibular ganglion begins to form by the coalescence of neural crest-derived precursors and entwine around the primary bud [39]. Likewise, angiogenesis is observed as new CD31-positive and VEGFR2-positive are present at the branch [32].

The glands develop actively and form secondary branches at E14 [31]. Acinar epithelial differentiation can be observed as aquaporin 5 (AQP5) positive cells start to be abundant [40]. KRT19⁺ duct cells and functional differentiation of acinar cells [30, 35] are detected at E15 [36]. Ascl3 transcription factor is also visible at E15 in the

ductal cells [41]. Ductal morphogenesis involves $KRT5^+$, Kit^+ , $KRT14^+$ cells, and such as surrounded by neurons [30]. At E16, alpha-smooth muscle actin-positive (α SMA $^+$) cells or myoepithelial cells, positive for p63, emerge. The MIST1 as a master regulatory of secretion is also expressed at E16 in the acinar cells [36]. At this time point, lumenization in the main duct occurs [31].

In adult salivary glands, SOX2 is necessary to preserve pluripotent stem cells. These SOX2 $^+$ cells are commonly found in the sublingual glands. Ascl3 is also located within the duct [30]. $KRT5^+$ cells are expressed in the glands postnatal. It is kept by parasympathetic innervation [42]. SOX10 is also expressed in the acinar mature salivary glands [43].

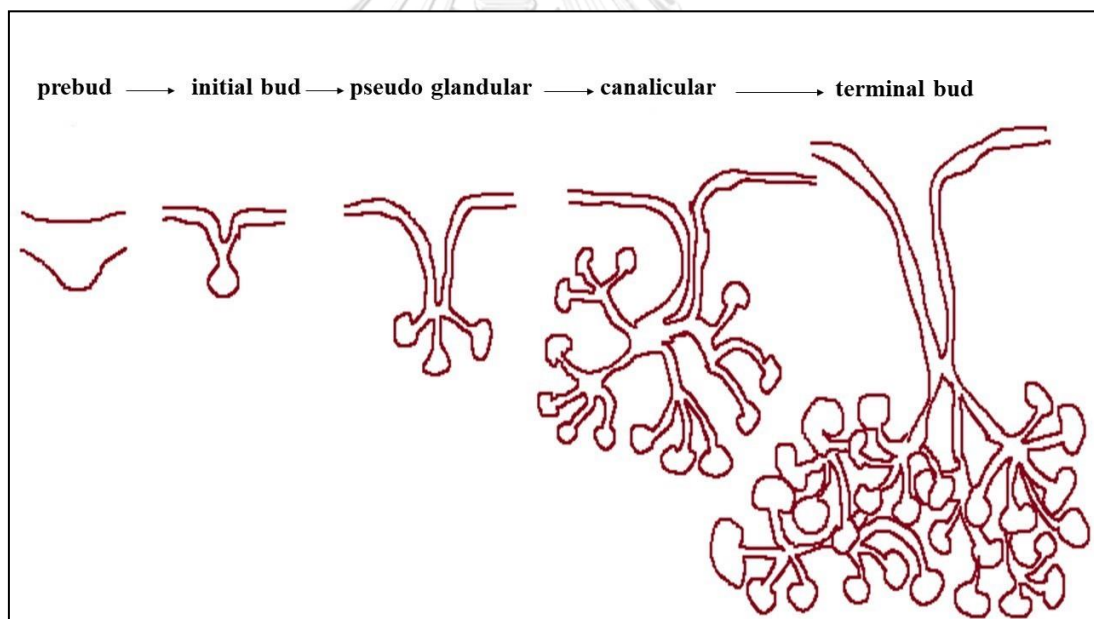


Figure 2.3. Stages of salivary gland development

2.2 Ionizing Radiation Principles

Any electromagnetic or particle radiation can transfer energy and generate an ion, named ionizing radiation [3]. As we know, the positively charged atomic nucleus is circled by the electrons, which are negatively charged. Thus, the atomic nucleus consists of the proton (positive charged) and neutron (neutral charged). The electrons are always in their orbital, maintained by electromagnetic force and the nuclei are strongly attached to each other supported by nuclear force [44].

At the specific isotope, nuclides are the nuclei of atoms. The nuclides are bound, either stable or unstable. The decay resulting from spontaneous unstable nuclides generates the emission of particle/ photon termed radioactive decay [44]. Briefly, radioactivity/radioactive decay when a parent nuclei emit a daughter/subatomic nuclei accompanied by releasing the energy [45].

Alpha (α) decay is the decay from the nuclei resulting in α particle, similar to the helium nucleus. The α particles are generated with energy along the parent nuclides decays to the lower energy state. Beta (β) decay is caused when the nuclei produce electron emission [45].

There is evidence in which an electron is taken by a nucleus while orbiting on its orbital. This electron will go to an excited state then return to the ground state while releasing a photon [45]. The emitted photon is categorized as electromagnetic energy, which is γ -rays or X-rays.

X-ray is an electromagnetic energy photon that has neutral ionizing radiation. X-ray does not originate from radioactive decay. X-ray is generated by the electron motion from a high to lower energy state [46]. First, to generate X-rays, it needs moving electron production. These moving electrons are focused on reaching the

targeting anode and when the electrons are close to the anode's nucleus, they decrease in speed upon collision of the anode. The moving electrons kick the electrons within the anode, then triggers electrons from high energy levels to fill the empty electron orbital upon by releasing the electromagnetic radiation, called X-rays photon [47].

2.3 Radiotherapy for HNC

Radiotherapy is done by placing the radiation source next to the tumor site [48]. Vary on the cancer type and the location, radiotherapy can be performed using one technique or combination. There are two types of radiotherapy based on the site of the radiation source; external beam radiation therapy and internal radiation therapy. External beam radiation therapy is a technique that sends high-energy rays from outside of the body to the tumor location. An advanced technique of external beam RT is Intensity-modulated radiotherapy (IMRT) which is a three-dimensional technology that allows the high dose region to correspond with the target precisely [3, 49] and thus provides better clinical outcome to the patients [50]. Besides, this technique is expected to reduce the adverse effect of radiotherapy on the normal tissue surrounding the tumor [51].

Nowadays, radiotherapy uses X-ray energy than γ -ray. Shortly, the X-ray is produced by converting the electron's kinetic energy, which is accelerated under the potential electrical field. Within the X-ray tube, the cathode is heated by filament current to produce electrons. This process is named thermionic emission. With the larger filament current, the cathode generates more heat and more electrons [5]. Electrons will be focused on the high voltage field (6MV), provided by the Linear Accelerator (LINAC). LINAC is an equipment where the electrons produced are accelerated and hit the bremsstrahlung tungsten as the anode where the photons of the

X-ray are generated [52]. The photons, then, are centered into a particular beam outline by the collimator [53]. The collimator is made from lead, is positioned at the output side of the X-ray tube. The X-ray will be orientated in a particular shape by the collimator before released to the tumor site [5]. The photon produced by the bremsstrahlung has equivalent energy to the electrons' maximum energy, hitting the bremsstrahlung [53].

The energy in wave and particle forms that is emitted from a matter is termed radiation. If sufficient enough to pull the electron out from atoms or molecules, this kind of energy is determined as ionizing radiation [54]. Irradiation dose is the amount of energy accumulated within the substance by ionizing radiation [55]. Gray (Gy) is the international standard unit of dose. One gray is the same as the 1 joule of energy absorbed by 1 kg of material [53].

A molecule hit by ionizing radiation will generate unpaired electrons due to ionization [56]. Any molecular species that stands independently with an unpaired electron, either one or more in its atomic orbital, is categorized as a free radical. A free radical tends to either donate or accept another unpaired electron from other molecules to stabilize the molecule. Its reactivity is related to its ability to take or give the free electron [57].

One group of free radicals is reactive oxygen species (ROS) [58]. Endogenous ROS is mainly formed within mitochondria [59] through mitochondrial respiration [59]. Exogenous ROS is produced by ionization within the cell. The radicals, such as Superoxide ($O_2^{\cdot-}$), Oxygen radical ($O_2^{2\cdot}$), Hydroxyl (OH^{\cdot}), Peroxyl radical (ROO^{\cdot}) are very reactive. Instead of them, hydrogen peroxide (H_2O_2), Ozone (O_3), and singlet

oxygen ($^1\text{O}_2$) are non-reactive, but their derivatives are free radicals through some reactions within the cell [60].

There are two examples of OH^* formation [57]:

- Single-electron oxidation of water: $\text{H}_2\text{O} \rightarrow \text{HO}^* + \text{H}^+ + \text{e}^-$
- Single-electron reduction of hydrogen peroxide: $\text{H}_2\text{O}_2 + \text{e}^- \rightarrow \text{HO}^* + \text{HO}^-$

Another reactions generate ROS [61]:

- $\text{O}_2 + \text{e}^- \rightarrow \text{}^*\text{O}_2^-$ (superoxide radical)
- $\text{O}_2 + \text{H}_2\text{O} \rightarrow \text{}^*\text{HO}_2 + \text{OH}^-$ (perhydroxyl radical)
- $\text{}^*\text{HO}_2 + \text{e}^- + \text{H}^+ \rightarrow \text{H}_2\text{O}_2$ (hydrogen peroxide)

ROS concentration at a low or moderate level is beneficial for the cell's physiological functions. But, ROS can cause oxidative stress at a higher level, which creates potential impairment to biomolecules [58]. Hydroxyl radical, an example, can react with the DNA and damage the heterocyclic DNA bases and sugar [62]. OH^* binds to the guanine base with the lowest reduction potential creates 8-hydroxyl-7,8-dihydroguan-8-yl radicals [63]. OH^* also can attach to adenine base and produces 8-oxo-7,8-dihydroadenine (8-oxoAde) and 4,6-diamino-5-formamidopyrimidine (Fapy-Ade) as the main products [62, 63].

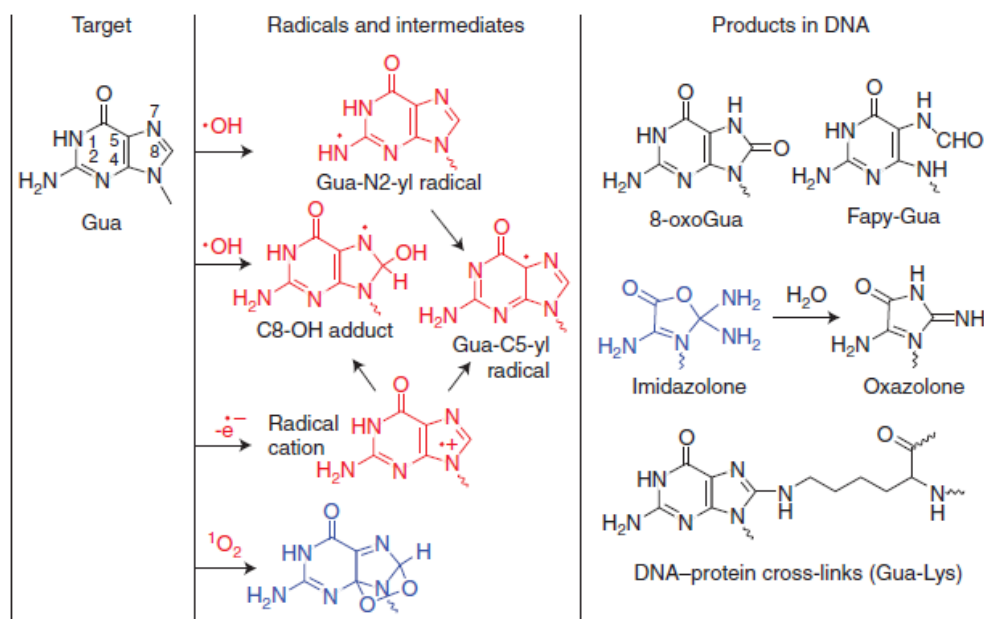


Figure 2.4. ROS and DNA binding [63]

ROS also affects lipid. It will cause lipid peroxidation, which ruins the membrane plasma functions. More severe, the end products from lipid peroxidation can cause DNA and protein damage, respectively [64]. Oxidation to the protein also occurs with the ROS existence. When protein reacts with ROS, amino acids within the protein are modified and lead to protein un-functional structure [65].

2.4 Current therapies to prevent radiotherapy damage -Amifostine

Prevention treatment is proposed to tackle radiation-induced xerostomia. There is only one drug approved by the Food and Drug Administration (FDA) as a cytoprotective drug from radiotherapy [19] and chemotherapy [66], named amifostine. Amifostine is a phosphorylated aminosulphydryl compound in the trihydrate form [67]. This drug is usually administrated intravenously [16] or subcutaneously [68]. Nowadays, it is widely used to avoid radiation-induced xerostomia [19].

Amifostine is delivered approximately 15-30 minutes before cancer therapy administration [16]. Alkaline phosphatase in the blood plasma, which highly presents in the normal tissue, nor the tumor tissue [69], will dephosphorylate amifostine into an active free sulfhydryl (thiol) metabolite. It works by facilitating electrostatic binding of the positive charge of amine groups to the negative charge within the DNA [70].

In vivo study of amifostine to irradiated mouse ovarian cell line resulted in p53 suppression [71]. As we know that p53 is a nuclear transcription factor that is responsible for such cellular processes; cell cycle arrest, senescence, and apoptotic. Activation of p53 can lead to those processes [72]. To undergo a normal cell cycle, p53 is must be in deficient levels [73].

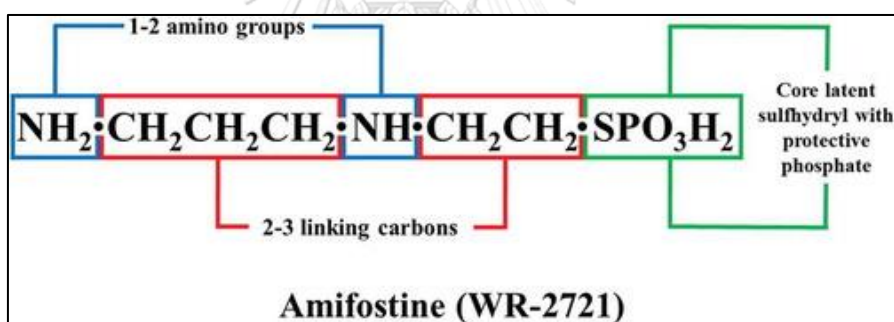


Figure 2.5. Structure of 2-(3-aminopropylamino) ethylsulfanyl-phosphonic acid or amifostine [67]

Amifostine was reported to decrease and delay mucositis and xerostomia related to radiotherapy in head and neck carcinoma patients [74, 75]. To the radiotherapy patients, amifostine resulted in better salivation and helped reducing xerostomia than non-amifostine patients [16, 76, 77].

Instead of its efficacy to protect cells from cancer therapy's effect, amifostine generates adverse effects such as hypotension, nausea, and vomiting [78]. This is one

of the reasons why antiemetic therapy is provided in parallel with amifostine treatment. Some patients also develop somnolence and sneezing [79]. Another limitation of this drug is the very narrow therapeutic window. The clearance of amifostine from blood plasma is 6 minutes, and the highest concentration of this drug within the tissue is only 10-30 minutes [18]. Therefore, frequent administration of this drug leads to severe side effects. Such severe side effects make patients interrupt its use and cause a delay in radiotherapy [20].

To treat post-radiation xerostomia in HNC patients, an FDA-approved drug named pilocarpine is commonly prescribed to stimulate saliva production by stimulating muscarinic receptors [80]. This drug is commonly delivered via systemic administration [81]. There are reports of succeeds increases unstimulated whole salivation [82, 83] and decreases the xerostomia severity up to 56% to HNC patients who undergo radiotherapy [84].

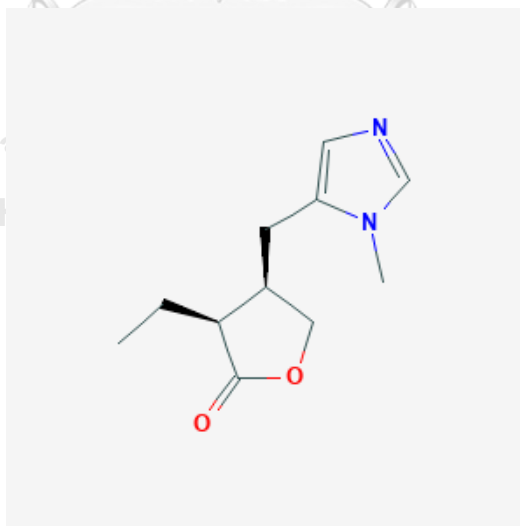


Figure 2.6. Structure of (3S,4R)-3-ethyl-4-[(3-methylimidazol-4-yl)methyl]oxolan-2-one or pilocarpine [67]

This drug is an alkaloid that acts as a cholinergic agonist [67]. It works by binding to any muscarinic receptors, which play-act upon the acetylcholine. Acetylcholine is the major neurotransmitter in the parasympathetic nervous system [85], which also innervates the salivary gland [86]. By stimulating the muscarinic receptor (M1 and M3 receptors), this means stimulating salivary exocrine organs [67]. Triggering the muscarinic receptor, in the acinar cells, it activates Ca^{2+} ion channel to increase the intracellular Ca^{2+} , stimulates basolateral K^{+} ion channel, and /or initiates apical Cl^{-} channels, respectively [87, 88]. Muscarinic receptor activation also drives water movement to the acinar cells via aquaporin 5 [89]. Thus, these processes lead to primary saliva production as the final result is the saliva secretion into the oral cavity [86]. Pilocarpine induction via M1 and M3 receptors is known to activate the ERK1/2 pathways [90], leading to aquaporin 5 activation [91].

Aside from pilocarpine effectiveness in promoting salivary production, this drug also exhibits side effects of systemic administration. Some articles reported that this drug intake is coupled with lacrimation, nausea, sweating, and increase in urine production [82, 92].

2.5. Epigallocatechin gallate

Polyphenols are secondary metabolites from plants with more than one phenolic ring without any nitrogen-based functional group [93]. Others classify polyphenols as non-volatile secondary plant metabolites that present one or more hydroxyl groups linked to the aromatic ring [94]. They can be divided into flavonoids and non-flavonoids. The flavonoids have two benzene rings as the backbone and a chain of three carbon atoms, linking the benzene rings [95].

Camelia sinensis is mainly known as a green tea herb and this plant provides leaves for the worldwide famous “healthy” green tea drink. It is made from the mature leaves of *Camelia sinensis* without the fermentation process and this makes the green tea drink preserve all its polyphenols [96].

The major constituent of green tea extract is epigallocatechin-3-gallate (EGCG) [21] which almost 50%-80% present in a cup of green tea [97]. Epigallocatechin gallate is a member of anthoxantins in the flavonoids group [98]. The presence of hydroxyl, methoxyl, and or glycosyl groups in flavonoids [99] offer antioxidant and chelating effect *in vitro* [100]. EGCG is soluble in water (33.3-100g/L) [98].

Catechin in green tea acts by chelating the metal ion, for example, iron (Fe^{2+}) and copper (Cu^{2+}) and by Fenton reaction, catechin avoids hydroxyl production. Therefore, EGCG by oral administration is relatively stable in the gastric and small intestine [98].

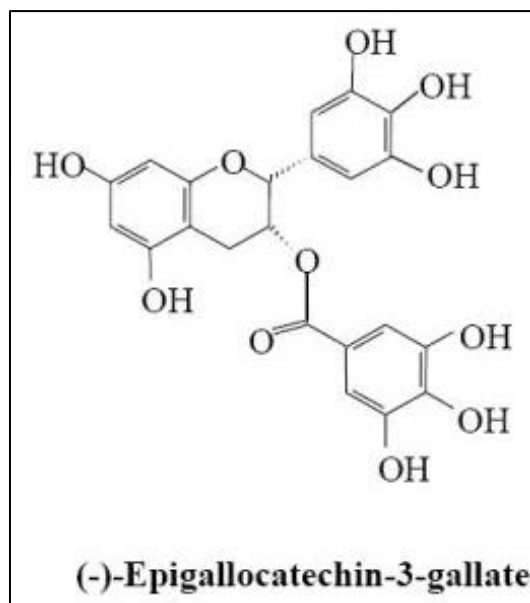


Figure 2.7. Epigallocatechin gallate (EGCG) structure [101].

EGCG also protected the immortalized epithelial SG cell lines *in vitro* from γ -rays by inhibition of p21 and p53 in an independent manner [22]. In addition, it increased the proliferation of those cell lines [22]. Furthermore, tea polyphenols pre-treatment to the γ -irradiated rats, *in vivo*, presented less the degranulation of the granular convoluted ductal cells and thus decreasing SG atrophy [102]. In our laboratory preliminary studies, EGCG pre-treatment to non-irradiated and irradiated salivary gland organs (with high energy photons) showed that EGCG could maintain epithelial growth and homeostasis (in non-irradiated glands) and protect the glands from damage (in irradiated glands).

A report showed that EGCG treatment *in vitro* of human breast epithelial enhances the antioxidant enzymes such as manganese superoxide dismutase and glutathione S-transferase [103]. Murine, fed a low dose of EGCG, generated elevation of peroxiredoxin 6 (PRDX6) and catalase [104]. Elevation of these enzymes related to the rising level of nuclear factor erythroid 2 (NFE2)-related factor 2 (Nrf2) within

the nucleus [103]. Nrf2 is a transcription factor responsible for antioxidant metabolizing enzyme production to eliminate free radicals [105]. In addition, EGCG also mediated AKT phosphorylation [103] which suppresses p53 activation [106]. Moreover, a decline of p38 MAPK was found in EGCG treatment to murine skin and human mammary epithelial cells and pancreatic cell lines [107, 108]. EGCG also induced Nrf2 level and its downstream antioxidant enzyme in mouse renal tubular epithelial cell study when the cells were triggered by ROS [109]. Aside from the increased level of Nrf2 activity, endothelial cell incubation with EGCG *in vitro* also showed PI3K/AKT and ERK1/2 pathways involvement [110].



3. Material and Methods

3.1 Salivary gland *ex vivo* culture

Animal procedures were utilized as per the approval by the Institutional Animal Care and Use Committee (IACUC) at the Chulalongkorn University Laboratory Animal Center protocol no. 1973004, and all experiments were conducted according to the guidelines of the Declaration of Helsinki and was approved by the Institutional Biosafety Committee of the Chulalongkorn University Faculty of Dentistry (Dent CU-IBC 006/2019 on March 2019 and DENT CU-IBC 006/2020 on March 2020.

Fetal mice at embryonic day E13.5-14 were selected from the ICR (*Mus musculus*) pregnant mouse. Submandibular glands (SMG) were dissected from ICR mouse embryos using microdissection under a stereomicroscope (SMZ1270i, Nikon, Japan) as described previously [111, 112].

After dissection, the fetal mice SMGs at embryonic day E.13.5-14 were cultured as previously described [113]. Briefly, the fetal mice SMG were cultured in dishes on polycarbonate membrane filters (Whatman™ Nucleopore™ Track-Etched Polycarbonate Membrane Filter, Sigma-Aldrich, St. Louis, MO, USA) at the air/medium interface, floated on the growth medium (GM) (DMEM/F-12 (Gibco, USA), 1% Penicillin/Streptomycin (Gibco, USA), 150 µg/mL ascorbic acid, and 100 µg/mL holo-transferrin (Gibco, USA). The SMGs were supplemented with EGCG (E4143-50M6, Sigma-Aldrich, USA) (7.5-30 µg/ml) for up to 72h in the incubator with 5% CO₂ and 37 °C. Positive controls had GM only. Every 24h 50% of the GM was removed and replaced with fresh GM. Glands were observed using brightfield

microscopy at 0h, 24h, 48h, and 72h to quantify the epithelial bud growth at 5-10x magnification with a DMi1 (Leica, Germany) (Figure 3.1A).

For the radiation injury experiment, at 24h, the glands of the treatment groups underwent irradiation generated by 6 MV Varian TrueBeam™ Linear Accelerator (Varian Medical System, Palo Alto, CA, USA), and they were cultured as described below (Figure 3.1B).

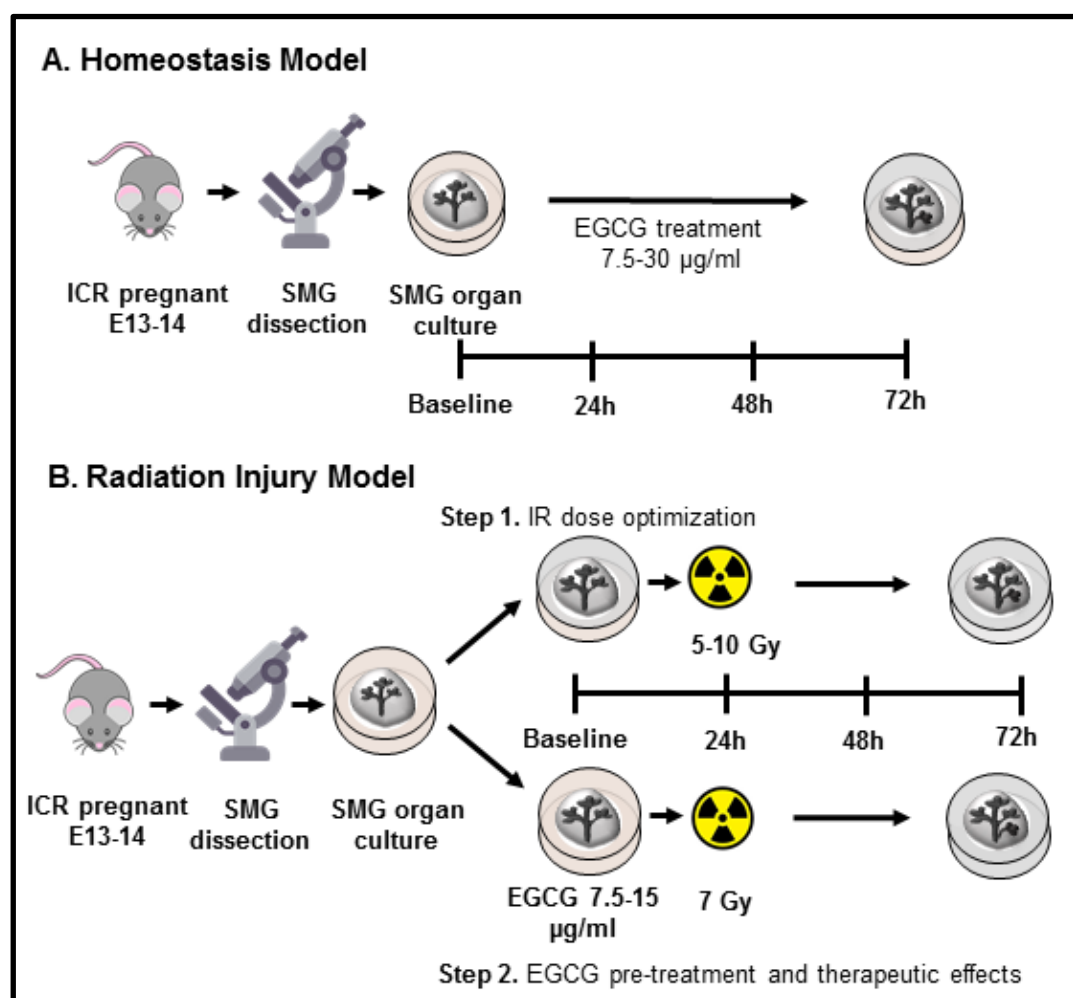


Figure 3.1. Methodology for the SG homeostasis and radiation injury models. (A) SMG organ culture with EGCG treatment during homeostasis. (B) SMG organ culture with radiation-induced injury with EGCG treatment.

3.2 Quantification of SMG Epithelial Growth

Epithelial salivary gland growth was quantified by counting the epithelial end buds using Image J (Bethesda, NIH, USA) cell counter in a blinded way after stripping off all treatment tags from the images. Epithelial growth index was quantified at different time points (baseline, 24, 48, and 72h) by normalizing the bud number at that time point to the bud number at the baseline. A comparison with the control treatment was carried out by dividing EGCG treated dishes with the control dishes. Each organ culture dish had three to four SMGs, and each treatment group was tested with up to three dishes. Each dish in the treatment group was run independently.

3.3 Quantitative real-time polymerase chain reaction

For all genomic expression studies, total ribonucleic acid (RNA) was extracted from baseline and 72h SMGs and DNase treated using Monarch[®] Total RNA Miniprep Kit (New England Biolabs, Hitchin, UK) for isolating the total RNA according to the manufacturer's protocol. Total extracted RNA was determined its purity and concentration used NanoDrop spectrophotometer (Thermo Fisher Scientific). Afterward, for synthesizing cDNA from total RNA, reverse transcriptase enzyme SuperScript[™] III First-Strand Synthesis System (Invitrogen[™], Thermo Fisher Scientific) was used and cDNA was diluted to 1 ng/ μ L in nuclease-free water. To perform SYBR-green-based qPCR, one ng of cDNA was used, primers were designed by Beacon Designer software (USA). Primers targeting proliferation, non-epithelial and epithelial stem cell, progenitor and differentiated markers for the SG were selected. The qPCR reaction in a total volume of 20 μ L consisting 10 μ L cDNA, 9.5 μ L QuantiTect SYBR[®] Green kit (QIAGEN, Hilden, Germany), 0.5 μ L of

forward, and reverse primer mix in a Applied Biosystems QuantStudio 3 Real-Time PCR system (ThermoFisher Scientific). Data was evaluated by $2^{-(\Delta\Delta CT)}$ method to quantify relative expression of target genes compared with reference housekeeping gene S-29 [114]. All oligonucleotide primers were confirmed in-house and checked for efficiency by serial dilution of cDNA. The primer sequences were used are as written in the supplementary section, Table 1.

The primer sequences used are as follows:

Table 1. List of oligonucleotide primer sequences

Gene	Forward	Reverse
<i>Ki-67</i>	CATACCTGAGCCCATCACCA	GCTGCATTCCGAGTA
<i>Sox 2</i>	CAGCATGTCCTACTCGCAGCAG	TGGAGTGGGAGGAAGAGGTAACC
<i>Krt14</i>	CAGCCCCTACTTCAAGACCA	GTCGATCTGCAGGAGGACAT
<i>Aqp5</i>	TCTACTTCTACTTGCTTTTCCCTCCTC	CGATGGTCTTCTTCCGCTCCTCTC
<i>Cdkn1a</i>	CCCCAATCGCAAGGATTCTT	CTTGGTTCGGTGGGTCTGTC
<i>Mist1</i>	GCTGACCGCCACCATACTTAC	TGTGTAGAGTAGCGTTGCAGG
<i>Krt19</i>	CCTCCCAGATTACAACCACT	GGCGAGCATTGTCAATCTGT
<i>Acta2</i>	GGAGAAGCCCAGCCAGTCGC	AGCCGGCCTTACAGAGCCCA
<i>Pecam1</i>	TCCAACAGAGCCAGCAGTATGAGG	TCCAATGACAACCACCGCAATGAG
<i>Tubb3</i>	CCAGAGCCATCTAGCTACTGACACTG	AGAGCCAAGTGGACTCACATGGAG
<i>Rsp29</i>	GGAGTCACCCACGGAAGTTCGG	GGAAGCACTGGCGGCACATG

3.4 Whole mount immunohistochemistry

After culturing for 72h, ex vivo SMGs were fixed using the 4% paraformaldehyde for 10min at room temperature then flipped the gland over and incubated again for a further 10min. SMGs were permeabilized with 0.1% Triton X-100 (Sigma-Aldrich, USA) for 15min then washed using 1x phosphate-buffered saline (PBS) three times. The tissues were blocked overnight with 10% donkey serum (Jackson Laboratories, ME, USA), 5% bovine serum albumin (BSA), and 1.8%

mouse on mouse (MOM) immunoglobulin G (IgG) blocking reagent (Vector Laboratories, CA) in 0.1% PBS-Tween 20. SMGs were incubated with the primary antibody overnight at 4 °C in the following ratios: mouse anti-Ki-67 (1:200, BD 556003), goat anti-Sox2 (1:100, Santa Cruz SC17320), rabbit anti-Krt14 (1:500, Abcam AB18595), rabbit anti-cleavage Caspase 3 (1:200, Cell Signaling), and β -3 Tubulin (1:100, R&D). Primary antibodies were detected with secondary antibodies AF488 chicken anti-mouse (1:200, Lifetech A21200), AF594 chicken anti-rabbit (1:200, Lifetech A21442), AF647 (:200, Lifetech A21236), and AF488 donkey-anti goat (1:100, Lifetech A11055). Nuclei were stained with Hoechst 33342 (1:1000, Invitrogen, R37605). All measurements used DMI8 Fluorescence Microscope (Leica), Zeiss LSM 700 (Germany), Zeiss LSM 900 (Germany), and processed by ZEN 3.0 (Zeiss, Germany). Quantification of fluorescence intensity used Image J software 2002 (Bethesda, NIH, USA).

Table 2. List of primary and secondary antibodies used in this study

	Antibody	Dilution	Manufacturer, Country/ Catalog Number
Conjugated Antibodies	Alexa Fluor 488	1:200	Thermo Fisher Scientific, USA/ A21200
	Alexa Fluor 594	1:200	Thermo Fisher Scientific, USA/ A21442
	Alexa Fluor 488	1:200	Thermo Fisher Scientific, USA/ A11055
Primary Antibodies	Sox 2	1:100	Santa Cruz, USA/ SC17320
	Ki67	1:200	Invitrogen, USA/ PA5-19462
	Krt14	1:500	Abcam, UK/ AB181595
	Cleaved Caspase 3	1:200	Cell Signalling Technologies/ USA, 9664S
	β -3 Tubulin	1:100	R&D system, USA/ MAB1195

3.5 Transmission electron microscopy

Ultrastructural analysis of intracellular secretory vesicles was initialized by fixing the 72h culture time SMGs with 3% glutaraldehyde in 0.1 M phosphate buffer. Tissues were rinsed in 0.1 M phosphate buffer for two min three times. In 2% osmium tetroxide (Sigma-Aldrich, USA) post-fixation process was done in the same buffer solution at 4 °C for 45min, and with a graded series of alcohol tissues were dehydrated then embedded in Spurr's resin: propylene oxide (1:1) for 10min, Spurr's resin: propylene oxide (3:1) for 15min, and 100% Spurr's resin for 15 minutes three times. The embedding process continued through 16h at 70 °C. Semi-thin sections were achieved using glass knives with Ultracut E Microtome (Leica Microsystems, Germany), and ultra-fine sections (90– 100 nm) were mounted on copper grids of 100

meshes. Uranyl acetate and lead were used to stain the grids before observing the grids using a transmission electron microscopy (JEM-1400, JEOL, USA) adjusted to 200 kV. SMG Non-IR tissues were used as positive controls.

3.6 Griess Assay

For reactive oxygen species, the Griess assay was performed to measure the amount of NO_2^- . Briefly, 50 μL of conditioned media (from glands from baseline and post-radiation after EGCG treatment) were placed into 96-well flat bottom plates and 50 μL sulfanilamide solution (G2930, Promega, US) was added and the mixture was incubated for 5-10 minutes at room temperature in a dark chamber. N-1-naphthylethylenediamine dihydrochloride (NED) solution (G2930, Promega, US) 50 μL was added subsequently, followed by incubation at room temperature for further 5-10 minutes. Pure nitrite solution was utilized to produce a standard curve. For subtracting the background levels of nitrites in the fresh media, fresh GM was used. The absorbance was measured within 30 minutes in a microplate reader (GloMax® Discover, Promega, US) at 490nm wavelength.

3.6 Data analysis

Data were plotted as mean \pm SEM. A normal distribution was identified, and hence we used unpaired *Welch's Student t*-test for two-group comparisons, and for more than two group- comparisons, one-way Anova with Tukey or Dunnet *post-hoc* analysis. The alpha level was set at 5% and thus $p < 0.05$ was considered significant. All statistical analyses were performed by Prism software version 8 (GraphPad Software, San Diego, CA, USA).

4. Results

4.1 Objective 1: Identify whether EGCG supports epithelial maintenance during salivary gland homeostasis.

4.1.1 Effect of EGCG on developing SG epithelial growth

When assessing the gland size, secondary epithelial duct formation and epithelial buds from baseline to 72h, EGCG at 7.5–15 $\mu\text{g/mL}$ supported both submandibular and sublingual epithelial growth (Figure 4.1A). In contrast, 30 $\mu\text{g/mL}$ EGCG showed a remarkably slower epithelial growth (Figure 4.1A). Further, the epithelial growth index indicated that EGCG 7.5–15 $\mu\text{g/mL}$ exponentially increased SG epithelial bud growth (Figure 4.1B). Meanwhile, EGCG 30 $\mu\text{g/mL}$ decreased the epithelial bud growth (Figure 4.1B). In comparison with other experimental doses, EGCG 7.5-15 $\mu\text{g/mL}$ showed a similar effect with control in supporting SG epithelial growth during 72h cultured time. At the same time, EGCG 30 $\mu\text{g/mL}$ showed less epithelial growth in a significant manner relative to other doses (Figure 4.1B). The expression of pro-mitotic marker *Ki67* was determined to evaluate whether EGCG affected cell mitosis in the SG (Figure 4.1C). The treatment with EGCG at 7.5–15 $\mu\text{g/mL}$ showed both epithelial bud proliferation and cellular mitosis comparable with the untreated gland undergoing regular homeostasis during *ex vivo* fetal development.

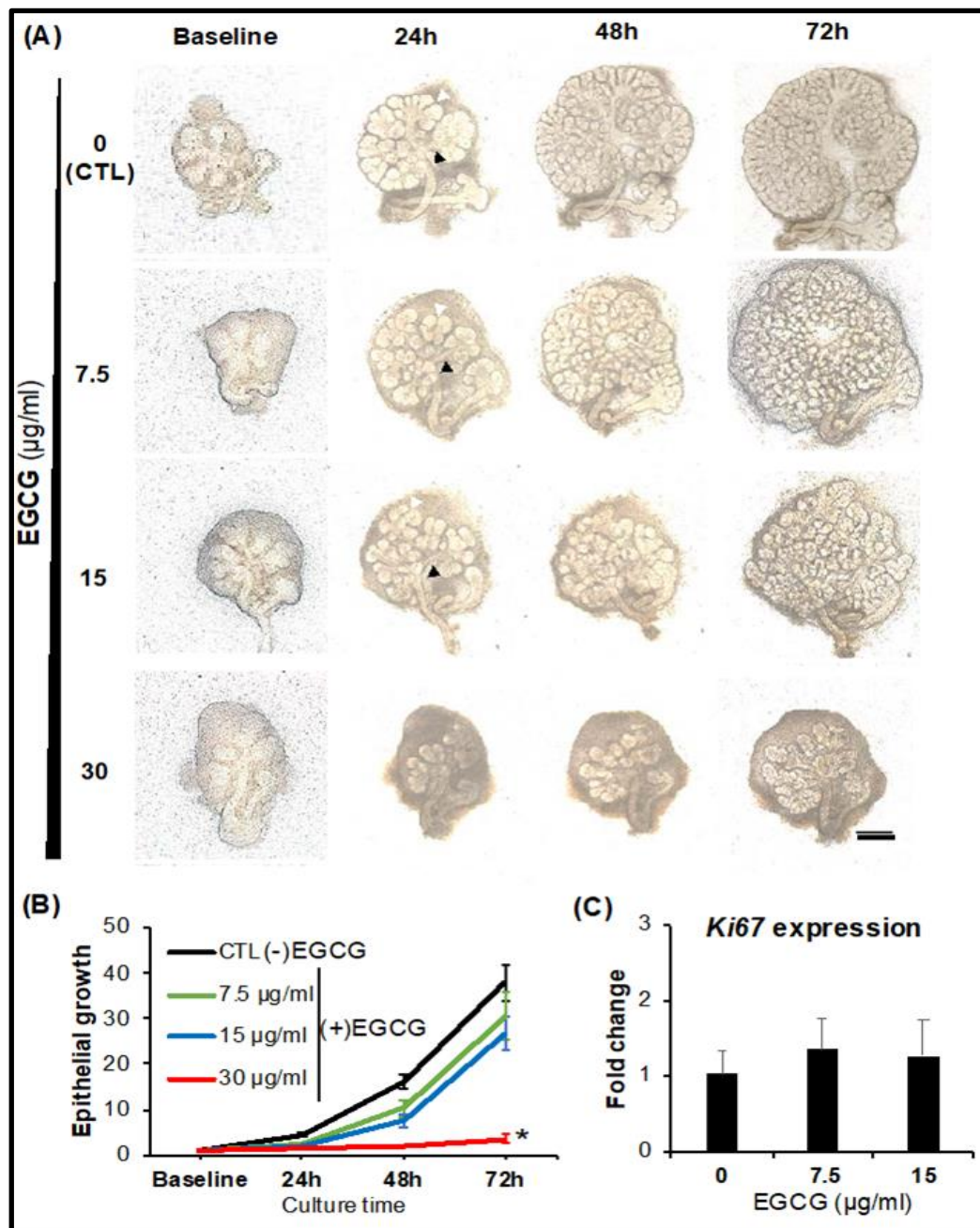


Figure 4.1. (A) Bright-field microscopy imaging of SG cultured with EGCG for 72h. Secondary duct formation is shown by black arrowheads. White arrowheads point to epithelial bud clefting. Max 4 \times . Scale bar: 200 μ m. (B) Quantification of SG epithelial growth when SG was treated with different EGCG concentrations. Error bars represent SEM from $n = 10-12$. * $p < 0.0001$ when compared to control by one-way ANOVA with Dunnett's *post-hoc* analysis. (C) Proliferation activity by measuring the expression of a mitotic marker at 72h. Y-axis represents the fold change

of *Mki67* gene relative to baseline levels and normalized to *Rsp29* (housekeeping gene). Error bars represent SEM from $n = 3$. One-way ANOVA with Tukey post hoc analysis revealed no significant differences.

4.1.2 Biological effects of EGCG on the expression of SG specific genes

Based on Figure 4.1 data, EGCG 7.5–15 $\mu\text{g/mL}$ had the ability to maintain SG epithelial growth. Thus, EGCG 7.5–15 $\mu\text{g/mL}$ was used to study such epithelial effects in the next experiments.

To determine the EGCG effects on SG gene expression, specific SG markers were evaluated by qPCR. *Sox2* and *Krt14* gene expression were evaluated to identify whether SG progenitor markers were influenced by EGCG treatment. Figure 4.2 showed that EGCG groups had similar effects relative to control (untreated glands).

To confirm the EGCG involvement in SG maturation, acinar SG, ductal SG, myoepithelial, neuronal, and vascular markers were assessed as seen in Figure 4.2. Regarding acinar differentiated markers like *AQP5* and *Mist1*, EGCG treatment groups showed comparable expression rates but slightly higher with *Mist1*. As for the ductal differentiated marker *Krt19*, EGCG treatments did not change its expression compared to untreated glands. Likewise, *Acta2*, a myoepithelial marker, was expressed similarly across all EGCG groups and untreated glands. Similarly, the expression of neuronal and vascular markers, *Tubb3* and *Pecam1*, respectively, did not change with EGCG treatment.

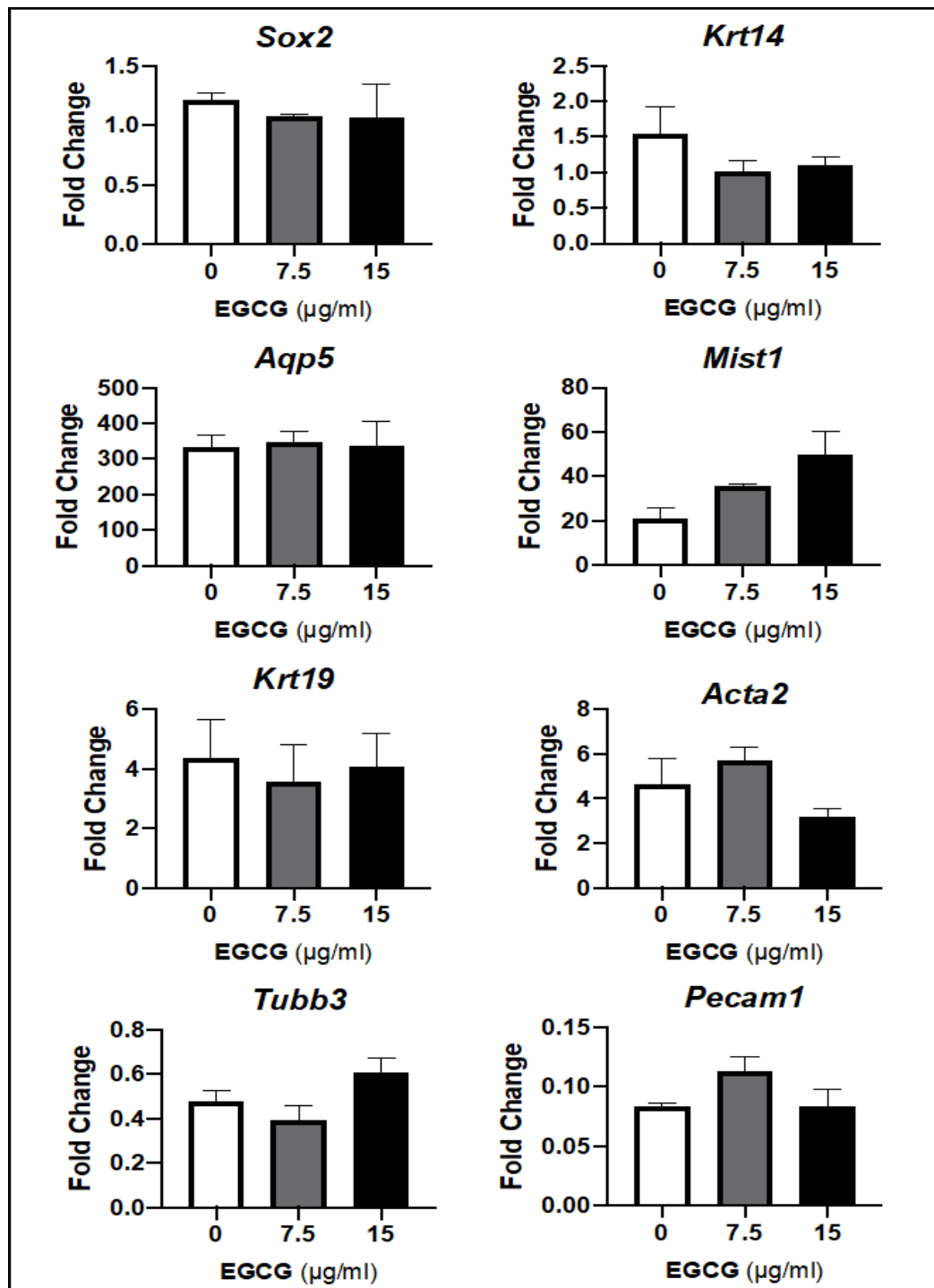


Figure 4.2. Gene expression of SG stem/progenitor cell, acinar and ductal epithelial, myoepithelial, neuronal, and vascular markers in the SG remains comparable with EGCG treatment at 7.5-15µg/mL concentrations. Y-axis represents fold change relative to baseline levels and normalized to *Rsp29* (housekeeping gene). Error bars represent SEM from $n = 3$, and each triplicate contains the RNA lysates of 3–4

glands. No statistically significant differences by one-way ANOVA with Tukey's *post hoc* analysis. *Sox2*: SRY (sex-determining region Y)-box 2; *Krt14*: Cytokeratin 14; *Aqp5*: Aquaporin 5; *Mist1*: Class A basic helix-loop-helix protein 15; *Krt19*: Cytokeratin 19; *Acta2*: actin alpha 2, smooth muscle; *Tubb3*: Tubulin Beta 3 Class III; *Pecam1*: Platelet and Endothelial Cell Adhesion Molecule 1.

4.2 Objective 2: Determine whether EGCG protects the salivary gland from epithelial injury induced by radiotherapy

4.2.1 Radiotherapy generated epithelial injury on developing SG

To determine the effects of conventional linear accelerator radiation on the SG, radiation injury experiments were conducted by targeting the SG with different irradiation (IR) doses (0–10 Gy). As expected, the highest IR dose suppressed epithelial growth, branching morphogenesis and the mitotic activity (Ki67+ cells) inducing more SG damage (Figure 4.3A-B). A significant epithelial injury was shown with 7 Gy and 10 Gy (Figure 4.3B). To avoid complete epithelial damage, the 7 Gy radiation dose was used for the final radiation injury model.

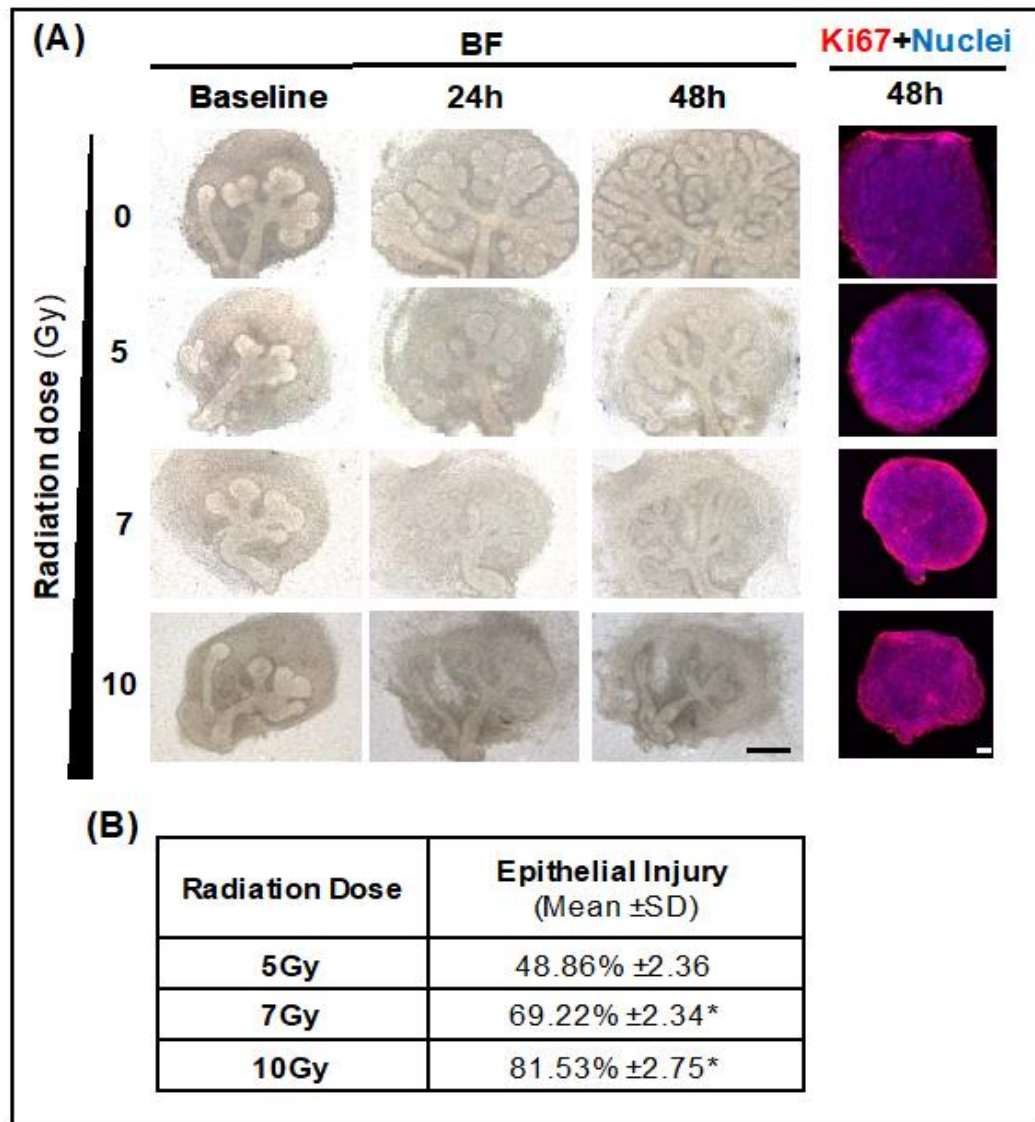


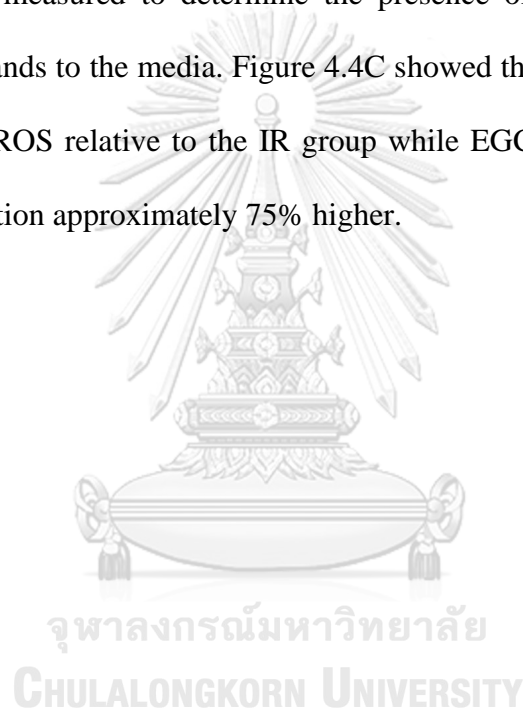
Figure 4.3. Determining optimal SG epithelial injury following LINAC radiation exposure in variation IR doses. (A) Bright-field (BF) and immunofluorescence imaging of SG stained by whole-mount immunohistochemistry for Ki67 mitotic marker and nuclei. Scale bar: 100 μ m. (B) Percentage of SG epithelial injury by increasing IR doses based on epithelial growth ratio for each dose and normalized to non-irradiated glands. Data are presented from n = 8–11. * p < 0.05 when compared to non-irradiated glands using one-way ANOVA with Dunnett's *post hoc* test.

4.2.2 EGCG protected SMG epithelial growth from radiation injury

SMG was cultured with different doses of EGCG 24h before IR time to identify whether EGCG could prevent radiation injury. These findings showed that

EGCG 7.5 $\mu\text{g}/\text{mL}$ prevented *ex vivo* SMG damage relative to the IR group (Figure 4.4A), as seen from the increase in gland size and number of epithelial buds. Epithelial bud growth quantification was performed and EGCG 7.5 $\mu\text{g}/\text{mL}$ showed significantly higher epithelial bud growth relative to the IR group. Conversely, other EGCG groups showed lower epithelial growth (Figure 4.4B).

Next, the production of reactive oxygen species (ROS) in the *in vitro* environment was measured to determine the presence of oxidative stress markers released by the glands to the media. Figure 4.4C showed that 7.5 $\mu\text{g}/\text{mL}$ EGCG could suppress 75% of ROS relative to the IR group while EGCG at 15 $\mu\text{g}/\text{mL}$ generated more ROS production approximately 75% higher.



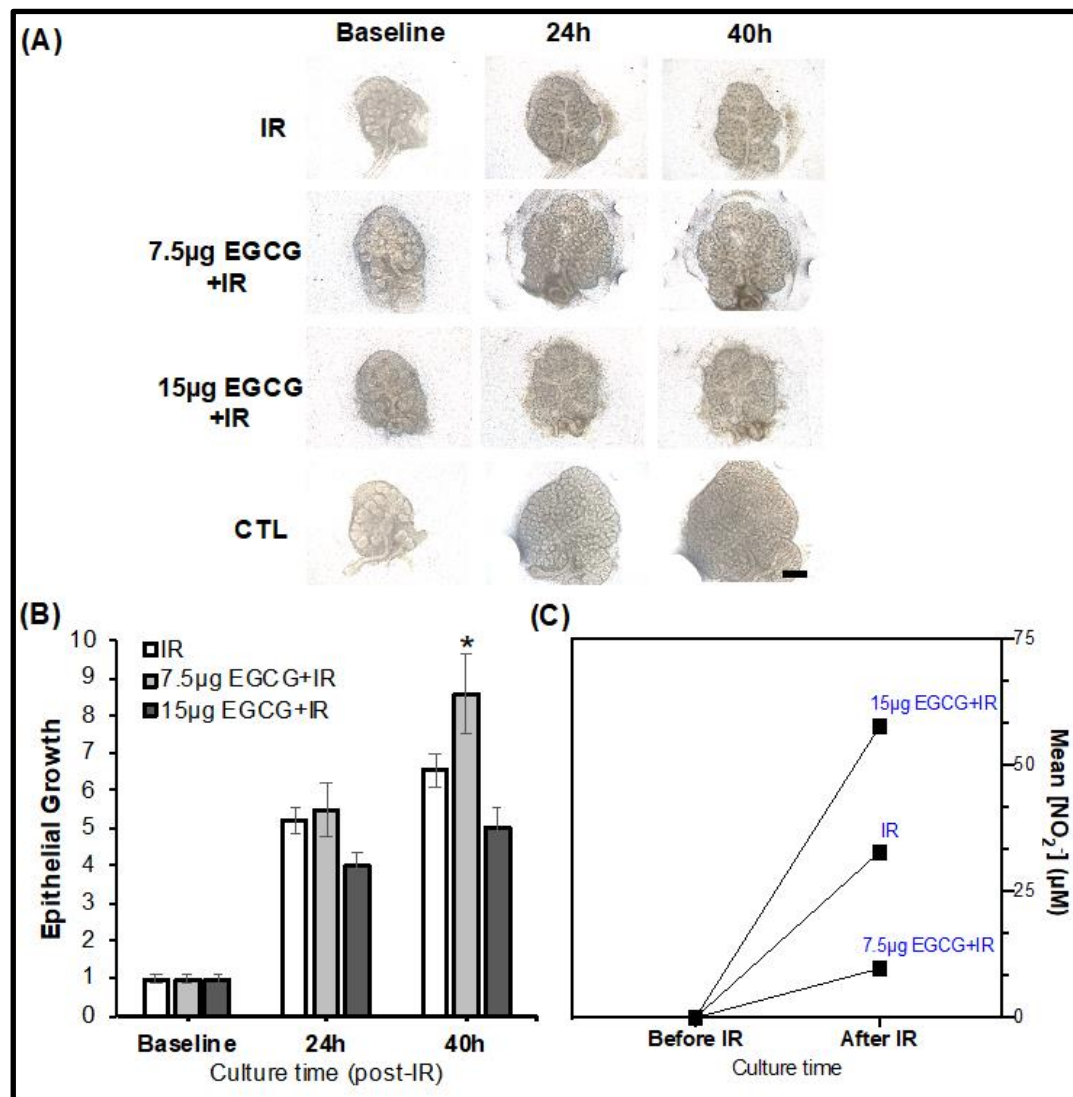


Figure 4.4. EGCG 7.5 µg/mL increased epithelial growth and decreased oxidative stress markers after IR injury. **(A)** Bright-field micrographs of SG treated with EGCG before IR injury. Mag.: 4×. Scale bar: 100 µm. **(B)** Quantification of epithelial growth ratio during culture with EGCG treatment. Error bars represent SEM from $n = 12-18$. * $p < 0.001$ when compared to IR using one-way ANOVA with Dunnett's *post hoc*. **(C)** Quantification of oxidative stress by determining the levels of nitrites (via a Griess assay) in conditioned media before and after IR and EGCG treatment of the injured SG.

4.2.4 EGCG protected SMG progenitor cells from radiation injury

Next, IHC for mitotic marker Ki67 and SG epithelial progenitor markers Sox2 and Krt14 was performed to identify the biological epithelial effects of EGCG after irradiation injury, particularly the mitotic activity and the presence of SG epithelial progenitor cells. Pro-acinar SMG buds in the EGCG pre-treated group significantly expressed more Sox2⁺ cells, KRT14⁺ cells, and Ki67⁺ cells relative to the IR group (Figure 4.5A, B). It was also observed that there was upregulation of Sox2⁺ cells, Krt14⁺ cells, and Ki67⁺ cells at the ductal compartment when compared to the IR control group (Figure 4.5C, D).

At the gene expression arrays in Figure 4.5E, when compared to the IR group, EGCG exhibited significant upregulation of *Aqp5* and *Mist1*, which are known mature acinar epithelial SG markers. It was also observed that EGCG upregulated the myoepithelial marker, *Acta2*, but no differences were found on the mature ductal marker *Nkcc1*.

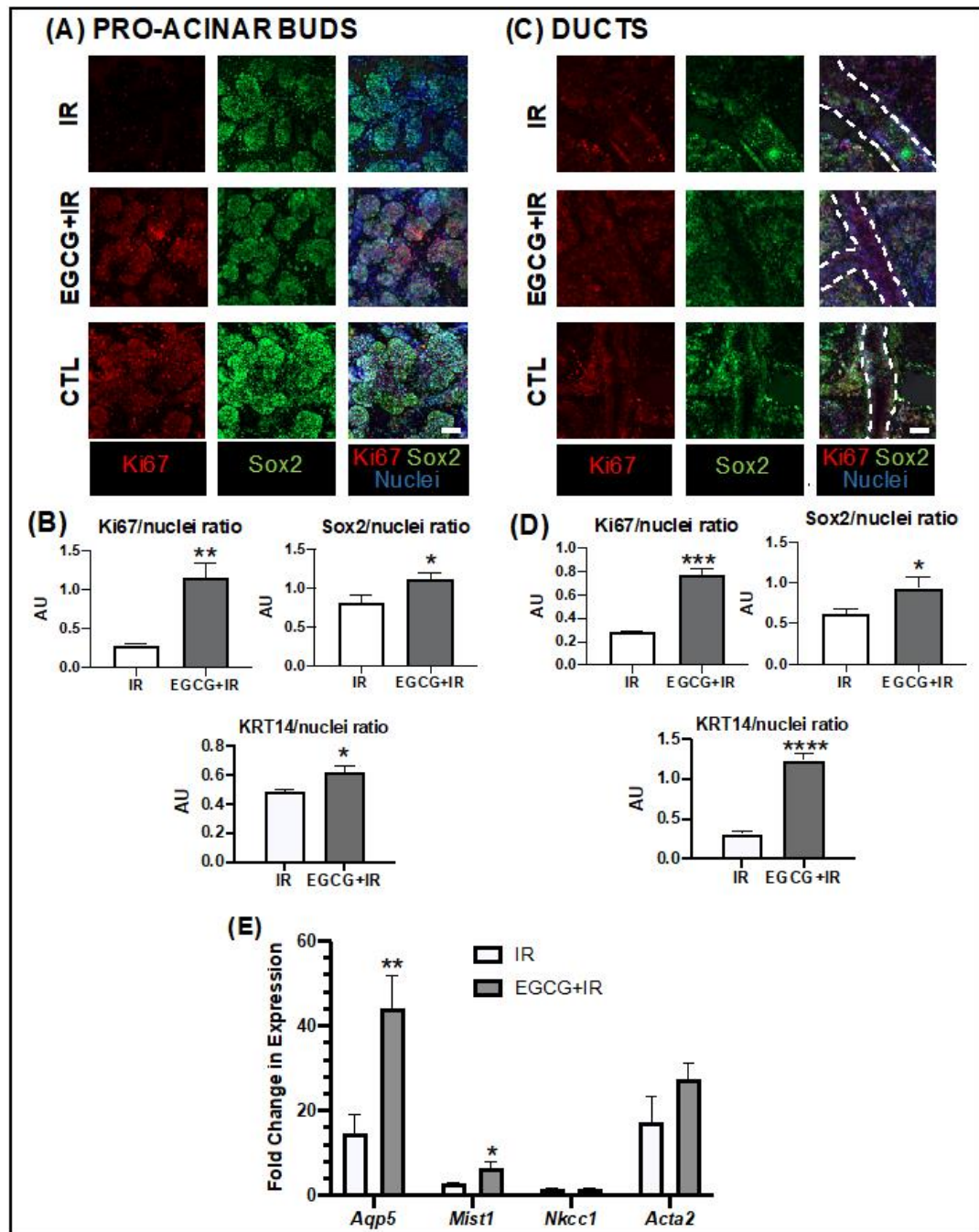


Figure 4.5. SMG endbud and ductal showed increasing of epithelial proliferation and epithelial markers with EGCG pre-treatment after IR injury. (A,C) Immunohistochemistry imaging of SMG pro-acinar (A) and ductal (C) after injury with EGCG 7.5 $\mu\text{g}/\text{mL}$ pre-treatment showed pro-mitosis cell marker (Ki-67) and SG epithelial stem cell marker, Sox2. The images shown are maximum intensity projections with their XYZ orthogonal projections. Nuclei are stained with Hoecht

33342. Non-irradiated CTL was used to confirm antibody immuno-reactivity. Mag.: 20×. Scale bar: 50 μm. (B,D) Graphs of Ki67, SOX2, and KRT14 quantification of based on the immunofluorescence signals at random ROI in pro-acinar buds (B) and ducts (D) and normalized to total nuclei. Error bars represent SEM from n = 5 ROI. Welch's Student t-test were performed between untreated and treated: * p < 0.05, ** p < 0.01, *** p < 0.001, **** p < 0.0001 (E) Myoepithelial, acinar and ductal epithelial differentiation markers expression of in the whole gland by qPCR. Data are presented as mean (n = 3) of fold change relative to housekeeping gene normalized to baseline. Error bars represent SEM from n = 3. Welch's Student's t-tests were performed between untreated and treated: * p < 0.05, ** p < 0.01.

In the heatmap panel with gene expression data in Fig 4.6, when compared with non-IR CTL glands, EGCG pre-treatment (EGCG+IR group) preserved SG epithelial progenitor markers *Sox10* and *Krt5*, which downregulate through culture as expected. A slight upregulation of SG ductal differentiated gene *Krt19* was found but no statistical difference between groups was present. The expression of neuronal (*Tubb3*) and vascular (*Pecam*) compartment genes decreased through culture, particularly *Pecam*, though no differences were found between groups.

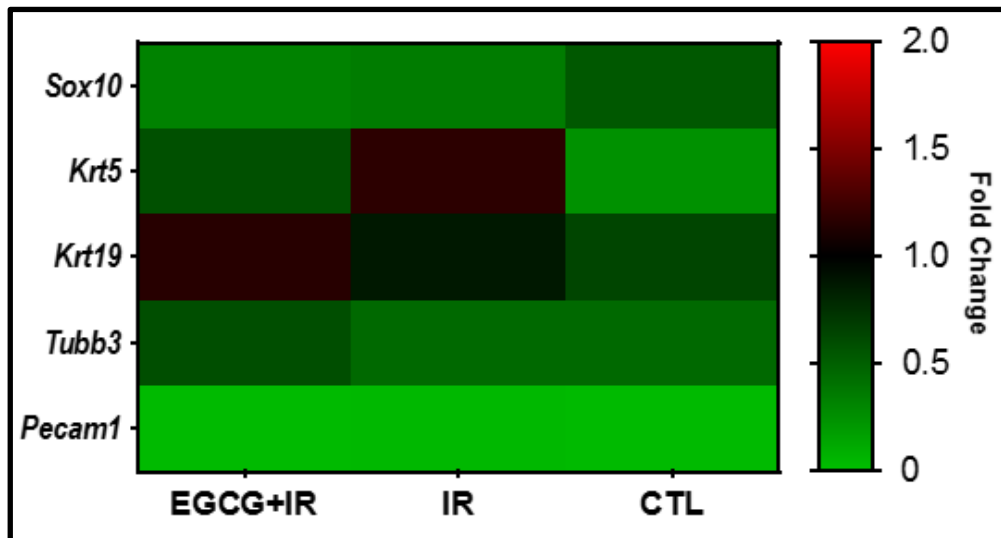


Figure 4.6. Heatmap expression of other stem/progenitors, ductal epithelial, neuronal and vascular markers from the whole gland by qPCR. Data are presented as mean (n = 3) of fold change relative to housekeeping gene normalized to baseline from n = 3. Welch's Student's t-test was performed between untreated and treated but no significant difference was observed. CTL represents non-irradiated untreated controls.

4.2.5 EGCG prevented SMG cell from apoptosis induced by radiotherapy

Next, whole-mount IHC with cleaved-Caspase 3 antibody was performed to confirm the effect of EGCG on the apoptotic activity of irradiated epithelial SMG buds, as observed in Figure 4.7. Nerves were stained with Tubb3 antibody to demarcate the buds. These findings showed that EGCG pre-treatment reduced Caspase 3 activity in the gland epithelial buds. The neuronal network appeared more prominent in the EGCG group; however, the expression of Tubb3 protein was not analyzed further and quantified.

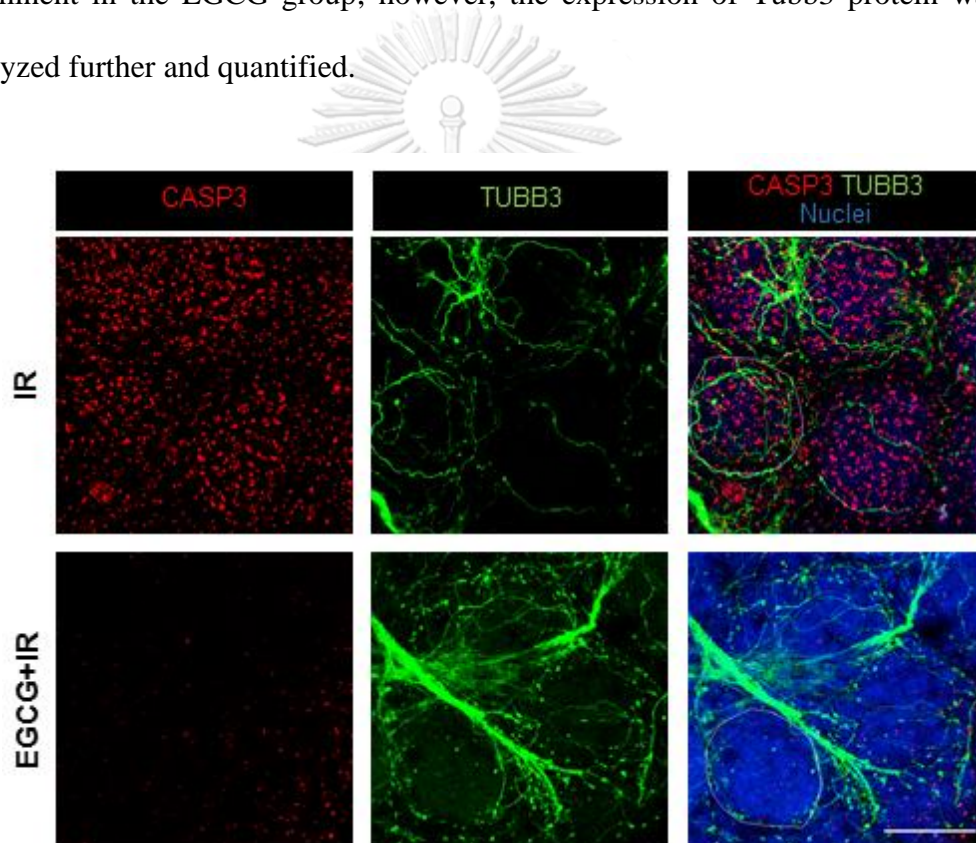


Figure 4.7. Expression of pro-apoptotic Caspase 3 marker in EGCG pre-treated glands after IR injury. SG was immuno-stained with cleaved-caspase 3 (CASP3), β -3 tubulin (TUBB3) to depict the boundaries of acinar buds where terminal neurons synapse. SG was also incubated with a nuclear stain. Mag.: 40X. Scale bar: 100 μ m.

Electron microscopy micrographs were taken to analyze further apoptosis's hallmarks in the epithelial buds (Figure 4.8). Micrographs indicated that IR glands

without treatment contained several apoptotic bodies (white arrows), while EGCG pre-treated glands showed significantly fewer apoptotic bodies. In addition, EGCG preserved the nuclear and plasma membranes in epithelial cells after irradiation.



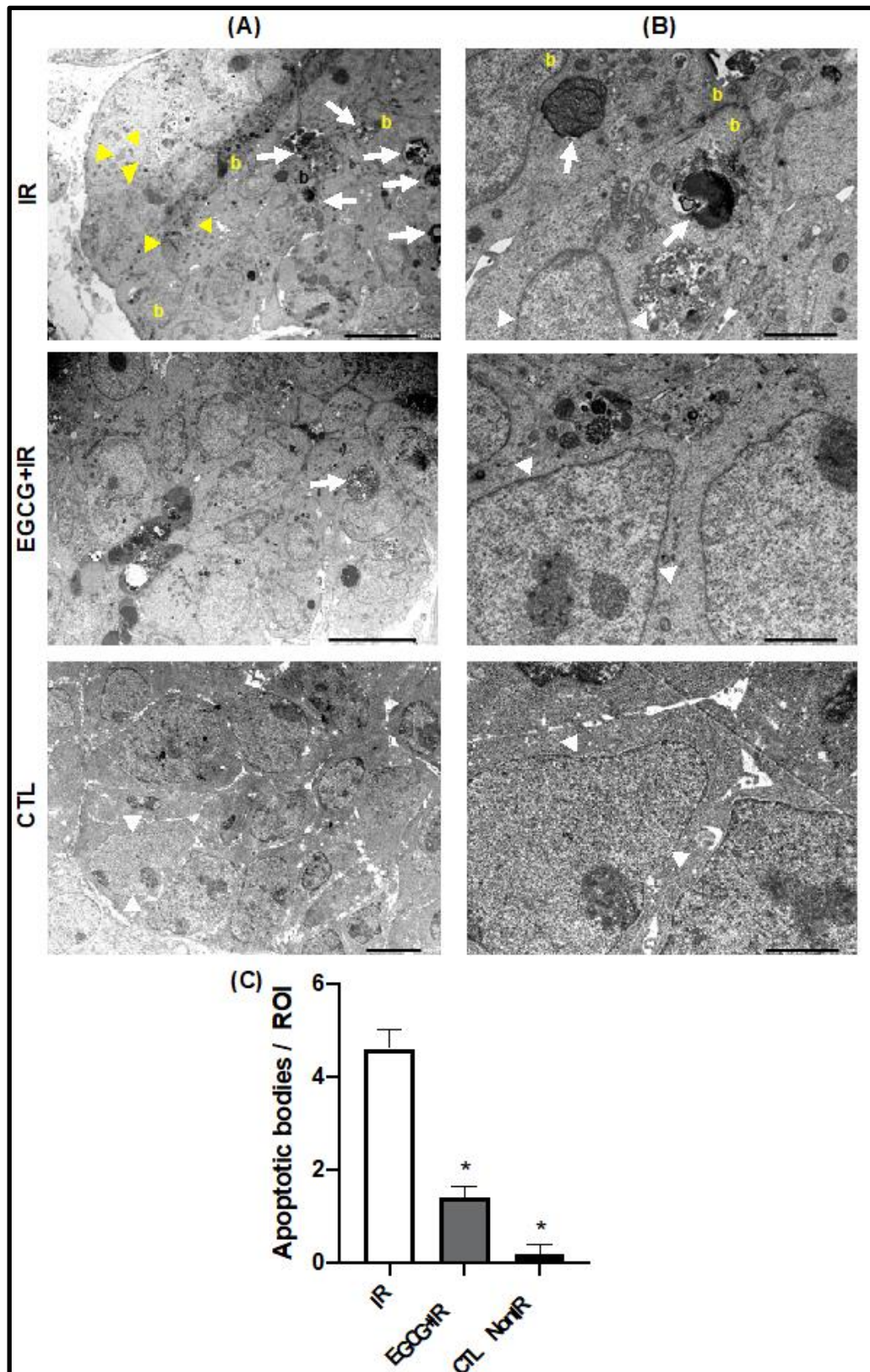


Figure 4.8. EGCG pre-treatment decreased IR-induced apoptosis and preserved typical nuclear organization. Transmission electron micrographs at low (**A panel**) and

high magnifications (**B panel**). Yellow arrowheads show nuclear chromatin fragmentation. White arrows depict apoptotic bodies. White arrowheads indicate the nuclear membrane borders. The yellow letter b represents membrane blebbing. (**C**) Apoptotic bodies were counted per region of interest (ROI) electron micrographs taken from in end bud regions with epithelial cells. Error bars represent SEM from $n = 5$. ANOVA with Dunnett's *post hoc* analysis was performed between IR and the other groups: * $p < 0.0001$.



5. Discussion and Conclusion

In this study, the antioxidant EGCG compound from green tea (*Camellia sinensis*) leaves was able to prevent radiation injury on *ex vivo* SMG model. In the *ex vivo* SG homeostasis experimental model, EGCG 7.5–15 $\mu\text{g/mL}$ exhibited exponential epithelial growth from baseline to 72h of culture, whereas 30 $\mu\text{g/mL}$ did not. This dose range was supported by a previous *in vitro* study where EGCG doses ranging from 5.7–23 $\mu\text{g/mL}$ (12.5–50 μM) maintained SG immortalized genetically modified cells [22]. In addition, in the same *in vitro* study, EGCG 5.7–23 $\mu\text{g/mL}$ supported acinar immortalized SG cell viability; however, 23 $\mu\text{g/mL}$ EGCG decreased immortalized ductal cell viability [22]. This latter finding support the fact that SG fetal epithelial growth at 15 $\mu\text{g/mL}$ EGCG in this study is less exponential than 7.5 $\mu\text{g/mL}$. However, the epithelial phenotypic findings were also supported by gene arrays where the expression of a pro-mitotic marker, *Ki67*, was comparable between the EGCG 7.5–15 $\mu\text{g/mL}$ groups and the untreated control group. Thus, EGCG at 7.5–15 $\mu\text{g/mL}$ does not affect epithelial proliferation and growth in the developing SG.

At the gene expression level, EGCG treatment groups exhibited comparable genotypic findings in term of *Sox2* and *Krt14*. *Sox2* is identified as a protein expressed by progenitors that generate both acinar and ductal compartment [35] and *Krt14* is established in ductal during development and take part in ductal formation and maintenance [115]. These imply that EGCG does not affect SG progenitor genes. The expression of SG mature epithelial genetic markers was evaluated to identify the effect on EGCG of the maturation SG epithelial progenitor cells. Regarding epithelial acinar cells, AQP5, which is identified as a water channel that mainly locates at the

apical membrane of mature acinar cells [116], and MIST1, a transcription factor required for exocytosis of acinar mature cells [117], were investigated. In EGCG treatment and untreated glands, *Aqp5* expression did not change through culture. Nevertheless, EGCG treatment enhanced the expression *Mist1*, although not significantly. Ductal *Krt19*, myoepithelial *Acta2*, neuronal *Tubb3*, and endothelial *Pecam1* are known SG markers [42, 118, 119], which were also assessed at the mRNA level to investigate the SG differentiated cells. Likewise, EGCG treatment did not affect *Krt19*, *Acta2*, *Tubb3*, and *Pecam1* and expression levels for these markers were comparable to the untreated glands. Taken together, these findings confirm that EGCG does not influence SG cell differentiation and maturation through regular development and homeostasis.

Next, a radiation injury model for the *ex vivo* fetal SG was successfully created for the first time with conventional LINAC-based radiation. In the present study, 7 Gy produced a significant SG epithelial injury. Due to irradiation (IR), the endogenous antioxidant function is impaired, upregulating ROS production and potentially causing epithelial injury to the glands [120]. In addition, excessive ROS has been reported to contribute to the decrease in SG stem cell progenitors on irradiated SMG and impairment to parasympathetic neuron ganglion and microvascular of endothelial cells [121-123]. Hence, radioprotectors are expected to tackle this radiation injury towards healthy SMG [124]. Protecting SMG from radiation damage is necessary due to its function to wet the oral cavity at rest [12]. Moreover, SMG is the second-largest salivary gland in humans and the largest salivary gland in mice [125, 126]. From previous studies, EGCG has shown its ability to exert antioxidant activity against IR damage [127-129]. Accordingly, this study

performed EGCG pre-treatment 24h before IR time to check EGCG ability to prevent SMG radiation injury. With EGCG pre-treatment, a significant enhancement of epithelial growth was shown by 7.5 $\mu\text{g/mL}$ EGCG which decreased a ROS marker, nitrite. Other studies have demonstrated that EGCG both at low and high doses (4.56-135.8 $\mu\text{g/mL}$; 23 $\mu\text{g/mL}$, respectively) can scavenge ROS on H_2O_2 -triggered mouse pancreatic and irradiated human epidermal keratinocyte cells resulting in lowering oxidative stress levels [108, 129]. Interestingly, Yamamoto et al [130] found that EGCG at 23-92 $\mu\text{g/mL}$ decreases ROS level on human epidermal keratinocytes and increased ROS on human oral squamous carcinoma cells. However, in future studies, others ROS markers such as H_2O_2 should be evaluated.

In line with EGCG's ability to decrease ROS production, EGCG provided a suitable environment that nourishes epithelial growth even after IR exposure. The increase of Ki67^+ cells found at pro-acinar and ductal SMG compartment with EGCG treatment in the present study reveals that EGCG treatment enhances the Ki67^+ cell population as found by Xie et al. in an *in vivo* mouse study looking at irradiated epithelial intestine cells pre-treated with 25 mg/kg EGCG [131]. In contrast, EGCG at 11.5-92 $\mu\text{g/mL}$ exerted cell viability inhibition toward oral cancer cells *in vitro*, while 11.5-23 $\mu\text{g/mL}$ in combination with 5-Fluorouracil reduced cancer cell migration [132]. Regarding epithelial stem/progenitor cells, Xie et al. also reported that enrichment of an intestinal stem cells population was observed upon the administration of 25 mg/kg of EGCG in 5 consecutive days before IR [131]. This evidence in epithelial stem cell population was also corroborated by this study as well. EGCG prevented the loss of progenitor cells in the irradiated SMG, which are Sox2 and KRT14, at both pro-acinar and ductal compartments.

This study also found an enhancement of acinar-related genes on the EGCG pre-treatment group compared to IR control. Significant upregulation of *Aqp5* and *Mist1* related genes with EGCG pre-treatment might be related to green tea ability to increase salivation either in xerostomia [133] and patients who underwent radioiodine treatment [134]. However, this salivary function is also supported by increasing ductal gene expression, as seen in Figure 4.14. An *in vivo* study revealed that delivering EGCG at 10 mg/kg improved vascular function and decreased inflammatory cytokine immediately after reperfusion injury caused by ROS [135]. This present study shows that EGCG polyphenol presented in green tea improves SG-related genes, even in a damaged SG.

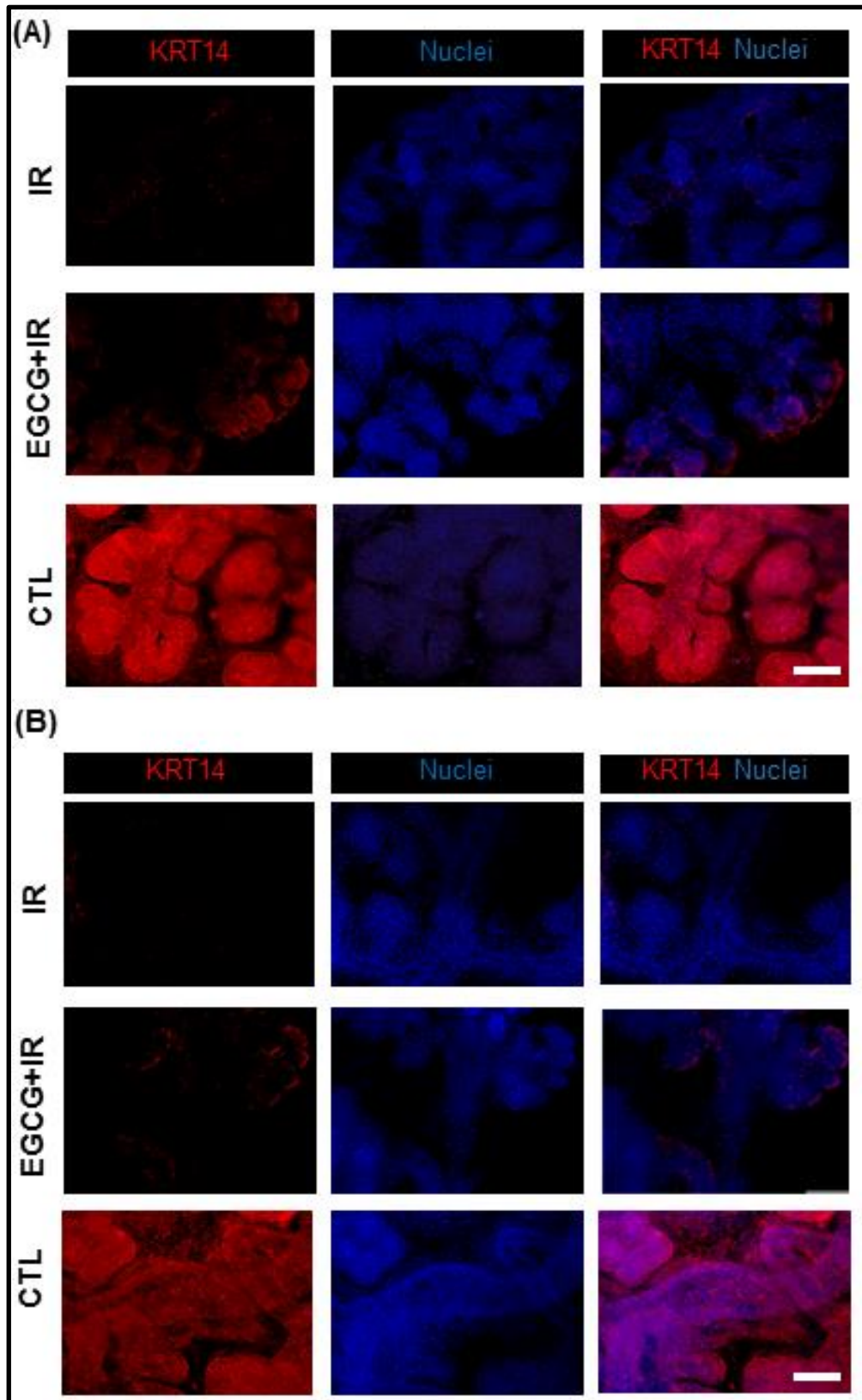
Ionizing radiation may generate cell death via apoptosis [136]. Increase of phosphorylated p53 with radiation treatment has been documented [137] and is linked with the upregulation of pro-apoptotic p53 target genes, such as p53 upregulated modulator of apoptosis (PUMA) [138] and increasing of Caspase 3 activity [137]. Apoptosis is recognized by generating a vehicle called apoptotic body as garbage sacks, which are then ingested by phagocytes [139]. In our study, with EGCG pre-treatment, less apoptotic bodies were expressed on irradiated SMG. This event indicated that EGCG prevents the SG cells from entering programmed cell death after IR. Future experiments using immunohistochemistry or Western blot to identify phosphorylated p53 are required to understand the apoptotic signaling pathway. In addition, further studies identifying antioxidant mechanisms are involved in the prevention of SG radiation-induced epithelial injury is also necessary. For example, assessing Nrf2 (nuclear factor erythroid 2-related factor) which is known to regulate the induction of genes encoding antioxidant proteins and phase 2 detoxifying enzymes

[140] is essential to confirm if EGCG influences Nrf2 nuclear translocation on regulating cellular antioxidant activity. Also, evaluating DNA damage is necessary since ionizing radiation alters the DNA structure [63, 141].

Furthermore, to confirm the beneficial effect of EGCG on preventing SG epithelial injury, *in vivo* experiments in mouse models are required to confirm the effectiveness of EGCG towards SG radiation injury prevention. EGCG is water-soluble and unstable, so one needs to develop techniques to enhance EGCG bioavailability and therapeutic potential when delivered as an intraoral drug. Some approaches were proposed, such as encapsulated EGCG in chitosan and loaded EGCG in lipid carriers which showed intestinal absorption enhancement [142, 143]. However, future studies will be needed to optimize the bioavailability of EGCG.

In conclusion, this study indicated that EGCG at 7.5 $\mu\text{g/mL}$ supported epithelial SG homeostasis during fetal gland development. In the SG injury model, EGCG protected the growth, mitosis, and maturation of the epithelia after radiation injury, generated a mature SG epithelial acinar and ductal compartment (genome and proteome levels), increased the epithelial stem cell niche (Sox2⁺), decreased radiation-induced cell apoptosis, and decrease oxidative stress markers in the SG organ culture.

Appendix Figure 1.



Appendix Figure 1. Expression of epithelial progenitors in EGCG-treated glands after IR injury. Expression of cytokeratin 14 (KRT14) progenitor markers in pro-acinar endbud compartments (A) and in ductal compartments (B) After immunofluorescence staining. Images shown are maximum intensity projections. Mag.: 20x. Scale bar: 100 μ m.



REFERENCES

1. WHO, *Estimated number of new cases in 2020, larynx, lip, oral cavity, nasopharynx, both sexes, all ages*. 2020.
2. Tangjaturonrasme, N., P. Vatanasapt, and A. Bychkov, *Epidemiology of head and neck cancer in Thailand*. Asia-Pacific Journal of Clinical Oncology, 2018. **14**(1): p. 16-22.
3. Baskar, R., et al., *Cancer and radiation therapy: current advances and future directions*. International journal of medical sciences, 2012. **9**(3): p. 193.
4. Tward, J.D., et al., *Radiation therapy and skin cancer*. Modern practices in radiation therapy, 2012: p. 207-246.
5. Seibert, J.A., *X-ray imaging physics for nuclear medicine technologists. Part 1: Basic principles of x-ray production*. Journal of nuclear medicine technology, 2004. **32**(3): p. 139-147.
6. Cho, B., *Intensity-modulated radiation therapy: a review with a physics perspective*. Radiation oncology journal, 2018. **36**(1): p. 1.
7. Barcellos-Hoff, M.H., C. Park, and E.G. Wright, *Radiation and the microenvironment–tumorigenesis and therapy*. Nature Reviews Cancer, 2005. **5**(11): p. 867-875.
8. Nagasawa, H. and J.B. Little, *Induction of sister chromatid exchanges by extremely low doses of α -particles*. Cancer research, 1992. **52**(22): p. 6394-6396.
9. Jensen, S., et al., *Xerostomia and hypofunction of the salivary glands in cancer therapy*. Supportive care in cancer, 2003. **11**(4): p. 207-225.
10. Grundmann, O., G. Mitchell, and K. Limesand, *Sensitivity of salivary glands to radiation: from animal models to therapies*. Journal of dental research, 2009. **88**(10): p. 894-903.
11. Lal, P., et al., *Changes in salivary flow rates in head and neck cancer after chemoradiotherapy*. 2010.
12. Jensen, S.B., et al., *A systematic review of salivary gland hypofunction and xerostomia induced by cancer therapies: prevalence, severity and impact on quality of life*. Supportive Care in Cancer, 2010. **18**(8): p. 1039-1060.
13. de Almeida, P.D.V., et al., *Saliva composition and functions: a comprehensive review*. J Contemp Dent Pract, 2008. **9**(3): p. 72-80.
14. Konings, A.W., R.P. Coppes, and A. Vissink, *On the mechanism of salivary gland radiosensitivity*. International Journal of Radiation Oncology* Biology* Physics, 2005. **62**(4): p. 1187-1194.
15. Koukourakis, M.I. *Amifostine: is there evidence of tumor protection? in Seminars in oncology*. 2003. Elsevier.
16. Brizel, D.M., et al., *Phase III randomized trial of amifostine as a radioprotector in head and neck cancer*. Journal of Clinical Oncology, 2000. **18**(19): p. 3339-3345.
17. Wasserman, T.H., et al., *Influence of intravenous amifostine on xerostomia, tumor control, and survival after radiotherapy for head-and-neck cancer: 2-year follow-up of a prospective, randomized, phase III trial*. International Journal of Radiation Oncology* Biology* Physics, 2005. **63**(4): p. 985-990.
18. Sriswasdi, C., S. Jootar, and F.J. Giles, *Amifostine and hematologic effects*. Journal of the Medical Association of Thailand= Chotmaihet thangphaet, 2000.

- 83(4):** p. 374-382.
19. Varghese, J., et al., *Localized delivery of amifostine enhances salivary gland radioprotection*. Journal of dental research, 2018. **97(11):** p. 1252-1259.
 20. Rades, D., et al., *Serious adverse effects of amifostine during radiotherapy in head and neck cancer patients*. Radiotherapy and Oncology, 2004. **70(3):** p. 261-264.
 21. Chu, C., et al., *Green tea extracts epigallocatechin-3-gallate for different treatments*. BioMed research international, 2017. **2017**.
 22. Yamamoto, T., et al., *Protective effects of EGCG on salivary gland cells treated with γ -radiation or cis-platinum (II) diammine dichloride*. Anticancer research, 2004. **24(5A):** p. 3065-3074.
 23. Tiwari, M., *Science behind human saliva*. Journal of natural science, biology, and medicine, 2011. **2(1):** p. 53.
 24. Proctor, G.B., *The physiology of salivary secretion*. Periodontology 2000, 2016. **70(1):** p. 11-25.
 25. Sneyd, J., E. Crampin, and D. Yule, *Multiscale modelling of saliva secretion*. Mathematical biosciences, 2014. **257:** p. 69-79.
 26. Amano, O., et al., *Anatomy and histology of rodent and human major salivary glands—Overview of the japan salivary gland society-sponsored workshop—*. Acta histochemica et cytochemica, 2012. **45(5):** p. 241-250.
 27. Ellis, H., *Anatomy of the salivary glands*. Surgery (Oxford), 2012. **30(11):** p. 569-572.
 28. Humphrey, S.P. and R.T. Williamson, *A review of saliva: normal composition, flow, and function*. The Journal of prosthetic dentistry, 2001. **85(2):** p. 162-169.
 29. Som, P. and I. Miletich, *The embryology of the salivary glands: an update*. Neurographics, 2015. **5(4):** p. 167-177.
 30. Patel, V.N. and M.P. Hoffman. *Salivary gland development: a template for regeneration*. in *Seminars in cell & developmental biology*. 2014. Elsevier.
 31. Patel, V.N., I.T. Rebutini, and M.P. Hoffman, *Salivary gland branching morphogenesis*. Differentiation, 2006. **74(7):** p. 349-364.
 32. Kwon, H.R., et al., *Endothelial cell regulation of salivary gland epithelial patterning*. Development, 2017. **144(2):** p. 211-220.
 33. Chatzeli, L., M. Gaete, and A.S. Tucker, *Fgf10 and Sox9 are essential for the establishment of distal progenitor cells during mouse salivary gland development*. Development, 2017. **144(12):** p. 2294-2305.
 34. Kwon, H.R. and M. Larsen, *The contribution of specific cell subpopulations to submandibular salivary gland branching morphogenesis*. Current opinion in genetics & development, 2015. **32:** p. 47-54.
 35. Emmerson, E., et al., *SOX2 regulates acinar cell development in the salivary gland*. Elife, 2017. **6:** p. e26620.
 36. Emmerson, E. and S.M. Knox, *Salivary gland stem cells: A review of development, regeneration and cancer*. genesis, 2018. **56(5):** p. e23211.
 37. Holmberg, K.V. and M.P. Hoffman, *Anatomy, biogenesis and regeneration of salivary glands*, in *Saliva: Secretion and Functions*. 2014, Karger Publishers. p. 1-13.
 38. Nedvetsky, P.I., et al., *Parasympathetic innervation regulates tubulogenesis in the developing salivary gland*. Developmental cell, 2014. **30(4):** p. 449-462.

39. Dyachuk, V., et al., *Parasympathetic neurons originate from nerve-associated peripheral glial progenitors*. Science, 2014. **345**(6192): p. 82-87.
40. Pin, C.L., et al., *The bHLH transcription factor Mist1 is required to maintain exocrine pancreas cell organization and acinar cell identity*. The Journal of cell biology, 2001. **155**(4): p. 519-530.
41. Lombaert, I. and M.P. Hoffman, *Stem cells in salivary gland development and regeneration*. Stem cells in craniofacial development and regeneration, 2013: p. 271-284.
42. Knox, S.M., et al., *Parasympathetic innervation maintains epithelial progenitor cells during salivary organogenesis*. Science, 2010. **329**(5999): p. 1645-1647.
43. Ohtomo, R., et al., *SOX10 is a novel marker of acinus and intercalated duct differentiation in salivary gland tumors: a clue to the histogenesis for tumor diagnosis*. Modern Pathology, 2013. **26**(8): p. 1041-1050.
44. Ojovan, M.I., W.E. Lee, and S.N. Kalmykov, *An introduction to nuclear waste immobilisation*. 2019: Elsevier.
45. Ahmed, S.N., *Physics and engineering of radiation detection*. 2007: Academic Press.
46. Albandar, H., *Basic Modes of Radioactive Decay*, in *Use of Gamma Radiation Techniques in Peaceful Applications*. 2019, IntechOpen.
47. Seibert, J.A. and J.M. Boone, *X-ray imaging physics for nuclear medicine technologists. Part 2: X-ray interactions and image formation*. Journal of nuclear medicine technology, 2005. **33**(1): p. 3-18.
48. Ajithkumar, T., *Principles of radiotherapy*. Specialist Training in Oncology E-Book, 2011: p. 15.
49. Bucci, M.K., A. Bevan, and M. Roach III, *Advances in radiation therapy: conventional to 3D, to IMRT, to 4D, and beyond*. CA: a cancer journal for clinicians, 2005. **55**(2): p. 117-134.
50. Luo, M.-S., G.-J. Huang, and H.-B. Liu, *Oncologic outcomes of IMRT versus CRT for nasopharyngeal carcinoma: A meta-analysis*. Medicine, 2019. **98**(24): p. e15951-e15951.
51. van Luijk, P., et al., *Sparing the region of the salivary gland containing stem cells preserves saliva production after radiotherapy for head and neck cancer*. Science translational medicine, 2015. **7**(305): p. 305ra147-305ra147.
52. Bourland, J.D., *Radiation oncology physics*, in *Clinical radiation oncology*. 2016, Elsevier. p. 93-147. e3.
53. Hodges, M. and A. Barzilov, *Radiation Safety Aspects of Linac Operation with Bremsstrahlung Converters*. Accelerator Physics: Radiation Safety and Applications, 2018: p. 123.
54. Miller, V., *Natural and Medical Radiation Dosages*. Physics.
55. L'Annunziata, M.F., *Radiation physics and radionuclide decay*, in *Handbook of Radioactivity Analysis*. 2012, Elsevier. p. 1-162.
56. Reisz, J.A., et al., *Effects of ionizing radiation on biological molecules—mechanisms of damage and emerging methods of detection*. Antioxidants & redox signaling, 2014. **21**(2): p. 260-292.
57. Riley, P., *Free radicals in biology: oxidative stress and the effects of ionizing radiation*. International journal of radiation biology, 1994. **65**(1): p. 27-33.
58. Phaniendra, A., D.B. Jestadi, and L. Periyasamy, *Free radicals: properties,*

- sources, targets, and their implication in various diseases.* Indian journal of clinical biochemistry, 2015. **30**(1): p. 11-26.
59. Khan, M.U., et al., *Generation of reactive oxygen species and their impact on the health related parameters: A critical review.* Int. J. Biosci, 2016. **9**: p. 303-323.
 60. Sharma, P., et al., *Reactive oxygen species, oxidative damage, and antioxidative defense mechanism in plants under stressful conditions.* Journal of botany, 2012. **2012**.
 61. Andrade Júnior, D.R.d., et al., *Oxygen free radicals and pulmonary disease.* Jornal Brasileiro De Pneumologia, 2005. **31**(1): p. 60-68.
 62. Dizdaroglu, M. and P. Jaruga, *Mechanisms of free radical-induced damage to DNA.* Free radical research, 2012. **46**(4): p. 382-419.
 63. Cadet, J. and J.R. Wagner, *DNA base damage by reactive oxygen species, oxidizing agents, and UV radiation.* Cold Spring Harbor perspectives in biology, 2013. **5**(2): p. a012559.
 64. Marnett, L.J., *Lipid peroxidation—DNA damage by malondialdehyde.* Mutation Research/Fundamental and Molecular Mechanisms of Mutagenesis, 1999. **424**(1-2): p. 83-95.
 65. Yan, L.J., *Analysis of oxidative modification of proteins.* Current protocols in protein science, 2009. **56**(1): p. 14.4. 1-14.4. 28.
 66. Santini, V., *Amifostine: chemotherapeutic and radiotherapeutic protective effects.* Expert opinion on pharmacotherapy, 2001. **2**(3): p. 479-489.
 67. Kim, S., et al., *PubChem 2019 update: improved access to chemical data.* Nucleic acids research, 2019. **47**(D1): p. D1102-D1109.
 68. Bardet, E., et al., *Subcutaneous compared with intravenous administration of amifostine in patients with head and neck cancer receiving radiotherapy: final results of the GORTEC2000-02 phase III randomized trial.* Journal of clinical oncology, 2011. **29**(2): p. 127-133.
 69. Singh, V.K. and T.M. Seed, *The efficacy and safety of amifostine for the acute radiation syndrome.* Expert opinion on drug safety, 2019. **18**(11): p. 1077-1090.
 70. Grdina, D.J., Y. Kataoka, and J.S. Murley, *Amifostine: mechanisms of action underlying cytoprotection and chemoprevention.* Drug metabolism and drug interactions, 2000. **16**(4): p. 237-280.
 71. YOON, Y.-D., et al., *Amifostine has an inhibitory effect on the radiation-induced p53-branched cascade in the immature mouse ovary. in vivo,* 2005. **19**(3): p. 509-514.
 72. Ozaki, T. and A. Nakagawara, *Role of p53 in cell death and human cancers.* Cancers, 2011. **3**(1): p. 994-1013.
 73. Kubbutat, M.H., S.N. Jones, and K.H. Vousden, *Regulation of p53 stability by Mdm2.* Nature, 1997. **387**(6630): p. 299-303.
 74. Patni, N., et al., *The role of amifostine in prophylaxis of radiotherapy induced mucositis and xerostomia in head and neck cancer.* Journal of Clinical Oncology, 2004. **22**(14_suppl): p. 5568-5568.
 75. Antonadou, D., et al., *Prophylactic use of amifostine to prevent radiochemotherapy-induced mucositis and xerostomia in head-and-neck cancer.* International Journal of Radiation Oncology* Biology* Physics, 2002. **52**(3): p. 739-747.

76. Nicolatou-Galitis, O., et al., *Oral candidiasis in head and neck cancer patients receiving radiotherapy with amifostine cytoprotection*. *Oral oncology*, 2003. **39**(4): p. 397-401.
77. Law, A., et al., *Efficacy and safety of subcutaneous amifostine in minimizing radiation-induced toxicities in patients receiving combined-modality treatment for squamous cell carcinoma of the head and neck*. *International Journal of Radiation Oncology* Biology* Physics*, 2007. **69**(5): p. 1361-1368.
78. Riley, P., et al., *Pharmacological interventions for preventing dry mouth and salivary gland dysfunction following radiotherapy*. *Cochrane Database of Systematic Reviews*, 2017(7).
79. Spencer, C.M. and K.L. Goa, *Amifostine*. *Drugs*, 1995. **50**(6): p. 1001-1031.
80. Millsop, J.W., E.A. Wang, and N. Fazel, *Etiology, evaluation, and management of xerostomia*. *Clinics in Dermatology*, 2017. **35**(5): p. 468-476.
81. Mercadante, V., et al., *Interventions for the management of radiotherapy-induced xerostomia and hyposalivation: A systematic review and meta-analysis*. *Oral oncology*, 2017. **66**: p. 64-74.
82. Yang, W.-f., et al., *Is pilocarpine effective in preventing radiation-induced xerostomia? A systematic review and meta-analysis*. *International Journal of Radiation Oncology* Biology* Physics*, 2016. **94**(3): p. 503-511.
83. Greenspan, D. and T.E. Daniels, *Effectiveness of pilocarpine in postradiation xerostomia*. *Cancer*, 1987. **59**(6): p. 1123-1125.
84. Nyárády, Z., et al., *A randomized study to assess the effectiveness of orally administered pilocarpine during and after radiotherapy of head and neck cancer*. *Anticancer research*, 2006. **26**(2B): p. 1557-1562.
85. Pakala, R.S. and K.N. Brown, *Cholinergic Medications*. 2019.
86. Pedersen, A.M.L., et al., *Salivary secretion in health and disease*. *Journal of Oral Rehabilitation*, 2018. **45**(9): p. 730-746.
87. Park, K., R.M. Case, and P.D. Brown, *Identification and regulation of K⁺ and Cl⁻ channels in human parotid acinar cells*. *Archives of Oral Biology*, 2001. **46**(9): p. 801-810.
88. Hayashi, T., et al., *The ACh-evoked, Ca²⁺-activated whole-cell K⁺ current in mouse mandibular secretory cells. Whole-cell and fluorescence studies*. *The Journal of membrane biology*, 1996. **152**(3): p. 253-259.
89. Ambudkar, I.S., *Ca²⁺ signaling and regulation of fluid secretion in salivary gland acinar cells*. *Cell calcium*, 2014. **55**(6): p. 297-305.
90. Lin, A.L., et al., *Distinct pathways of ERK activation by the muscarinic agonists pilocarpine and carbachol in a human salivary cell line*. *American Journal of Physiology-Cell Physiology*, 2008. **294**(6): p. C1454-C1464.
91. Hoffert, J.D., et al., *Hypertonic induction of aquaporin-5 expression through an ERK-dependent pathway*. *Journal of Biological Chemistry*, 2000. **275**(12): p. 9070-9077.
92. Aframian, D., et al., *Pilocarpine treatment in a mixed cohort of xerostomic patients*. *Oral Diseases*, 2007. **13**(1): p. 88-92.
93. Quideau, S., et al., *Plant polyphenols: chemical properties, biological activities, and synthesis*. *Angewandte Chemie International Edition*, 2011. **50**(3): p. 586-621.
94. Ottaway, P.B., *Food fortification and supplementation: Technological, safety*

- and regulatory aspects*. 2008: Elsevier.
95. Moreno, J. and R. Peinado, *Enological chemistry*. 2012: Academic Press.
 96. Cabrera, C., R. Artacho, and R. Giménez, *Beneficial effects of green tea—a review*. Journal of the American College of Nutrition, 2006. **25**(2): p. 79-99.
 97. Khan, N., et al., *Targeting multiple signaling pathways by green tea polyphenol (–)-epigallocatechin-3-gallate*. Cancer research, 2006. **66**(5): p. 2500-2505.
 98. Ramassamy, C., *Emerging role of polyphenolic compounds in the treatment of neurodegenerative diseases: a review of their intracellular targets*. European journal of pharmacology, 2006. **545**(1): p. 51-64.
 99. Choi, D.-Y., et al., *Antioxidant properties of natural polyphenols and their therapeutic potentials for Alzheimer's disease*. Brain research bulletin, 2012. **87**(2-3): p. 144-153.
 100. Corcoran, M.P., D.L. McKay, and J.B. Blumberg, *Flavonoid basics: chemistry, sources, mechanisms of action, and safety*. Journal of Nutrition in Gerontology and Geriatrics, 2012. **31**(3): p. 176-189.
 101. Singh, B.N., S. Shankar, and R.K. Srivastava, *Green tea catechin, epigallocatechin-3-gallate (EGCG): mechanisms, perspectives and clinical applications*. Biochemical pharmacology, 2011. **82**(12): p. 1807-1821.
 102. Peng, Z., et al., *Tea polyphenols protect against irradiation-induced injury in submandibular glands' cells: a preliminary study*. Archives of oral biology, 2011. **56**(8): p. 738-743.
 103. Na, H.-K. and Y.-J. Surh, *EGCG upregulates phase-2 detoxifying and antioxidant enzymes via the Nrf2 signaling pathway in human breast epithelial cells*. 2005. **65**.
 104. Dickinson, D., et al., *Epigallocatechin-3-gallate modulates anti-oxidant defense enzyme expression in murine submandibular and pancreatic exocrine gland cells and human HSG cells*. Autoimmunity, 2014. **47**(3): p. 177-184.
 105. Itoh, K., et al., *An Nrf2/small Maf heterodimer mediates the induction of phase II detoxifying enzyme genes through antioxidant response elements*. Biochemical and biophysical research communications, 1997. **236**(2): p. 313-322.
 106. Hu, W., Z. Feng, and A.J. Levine, *The regulation of multiple p53 stress responses is mediated through MDM2*. Genes & cancer, 2012. **3**(3-4): p. 199-208.
 107. Kundu, J.K., et al., *Inhibition of Phorbol Ester–Induced COX-2 Expression by Epigallocatechin Gallate in Mouse Skin and Cultured Human Mammary Epithelial Cells*. The Journal of Nutrition, 2003. **133**(11): p. 3805S-3810S.
 108. Cao, T., et al., *Antioxidant effects of epigallocatechin-3-gallate on the aTC1-6 pancreatic alpha cell line*. Biochemical and Biophysical Research Communications, 2018. **495**(1): p. 693-699.
 109. Du, X., et al., *Impact of epigallocatechin-3-gallate on expression of nuclear factor erythroid 2-related factor 2 and γ -glutamyl cysteine synthetase genes in oxidative stress-induced mouse renal tubular epithelial cells*. Molecular medicine reports, 2018. **17**(6): p. 7952-7958.
 110. Wu, C., et al., *Upregulation of heme oxygenase-1 by Epigallocatechin-3-gallate via the phosphatidylinositol 3-kinase/Akt and ERK pathways*. Life sciences, 2006. **78**(25): p. 2889-2897.
 111. Ferreira, J.N., et al., *Neurturin gene therapy protects parasympathetic function*

- to prevent irradiation-induced murine salivary gland hypofunction. *Molecular Therapy-Methods & Clinical Development*, 2018. **9**: p. 172-180.
112. Adine, C., et al., *Engineering innervated secretory epithelial organoids by magnetic three-dimensional bioprinting for stimulating epithelial growth in salivary glands*. *Biomaterials*, 2018. **180**: p. 52-66.
 113. Steinberg, Z., et al., *FGFR2b signaling regulates ex vivo submandibular gland epithelial cell proliferation and branching morphogenesis*. 2005. **132**(6): p. 1223-1234.
 114. Bookout, A.L. and D.J. Mangelsdorf, *Quantitative real-time PCR protocol for analysis of nuclear receptor signaling pathways*. *Nuclear receptor signaling*, 2003. **1**(1): p. nrs. 01012.
 115. Kwak, M., N. Alston, and S. Ghazizadeh, *Identification of Stem Cells in the Secretory Complex of Salivary Glands*. *J Dent Res*, 2016. **95**(7): p. 776-83.
 116. Matsuzaki, T., et al., *Function of the membrane water channel aquaporin-5 in the salivary gland*. *Acta histochemica et cytochemica*, 2012. **45**(5): p. 251-259.
 117. Hsieh, M.S., Y.M. Jeng, and Y.H. Lee, *Mist1: a novel nuclear marker for acinic cell carcinoma of the salivary gland*. *Virchows Arch*, 2019. **475**(5): p. 617-624.
 118. Karimi, A. and D.M. Milewicz, *Structure of the Elastin-Contractile Units in the Thoracic Aorta and How Genes That Cause Thoracic Aortic Aneurysms and Dissections Disrupt This Structure*. *Canadian Journal of Cardiology*, 2016. **32**(1): p. 26-34.
 119. Hauser, B.R., et al., *Generation of a Single-Cell RNAseq Atlas of Murine Salivary Gland Development*. 2020. **23**(12): p. 101838.
 120. Jasmer, K.J., et al., *Radiation-Induced Salivary Gland Dysfunction: Mechanisms, Therapeutics and Future Directions*. *Journal of Clinical Medicine*, 2020. **9**(12): p. 4095.
 121. Knox, S.M., et al., *Parasympathetic stimulation improves epithelial organ regeneration*. *Nature communications*, 2013. **4**: p. 1494-1494.
 122. Cotrim, A.P., et al., *Prevention of Irradiation-induced Salivary Hypofunction by Microvessel Protection in Mouse Salivary Glands*. *Molecular Therapy*, 2007. **15**(12): p. 2101-2106.
 123. Pringle, S., et al., *Human salivary gland stem cells functionally restore radiation damaged salivary glands*. *Stem cells*, 2016. **34**(3): p. 640-652.
 124. Jensen, S.B., et al., *Salivary Gland Hypofunction and Xerostomia in Head and Neck Radiation Patients*. *JNCI Monographs*, 2019. **2019**(53).
 125. Holsinger, F.C. and D.T. Bui, *Anatomy, function, and evaluation of the salivary glands*, in *Salivary gland disorders*. 2007, Springer. p. 1-16.
 126. Treuting, P.M. and S.M. Dintzis, *8 - Salivary Glands*, in *Comparative Anatomy and Histology*, P.M. Treuting and S.M. Dintzis, Editors. 2012, Academic Press: San Diego. p. 111-120.
 127. Yi, J., et al., *Radioprotection of EGCG based on immunoregulatory effect and antioxidant activity against 60Co γ radiation-induced injury in mice*. *Food and Chemical Toxicology*, 2020. **135**: p. 111051.
 128. Liu, G., et al., *Research of radioprotection of EGCG*. *Journal of Radiation Research and Radiation Processing*, 2002. **20**(2): p. 87-92.
 129. Zhu, W., et al., *Epigallocatechin-3-gallate (EGCG) protects skin cells from ionizing radiation via heme oxygenase-1 (HO-1) overexpression*. *J Radiat Res*,

2014. **55**(6): p. 1056-65.
130. Yamamoto, T., et al., *Green Tea Polyphenol Causes Differential Oxidative Environments in Tumor versus Normal Epithelial Cells*. Journal of Pharmacology and Experimental Therapeutics, 2003. **307**(1): p. 230.
 131. Xie, L.-W., et al., *Green tea derivative (-)-epigallocatechin-3-gallate (EGCG) confers protection against ionizing radiation-induced intestinal epithelial cell death both in vitro and in vivo*. Free Radical Biology and Medicine, 2020. **161**: p. 175-186.
 132. López, E.P.-F., F.G. García, and P.L. Jornet, *Combination of 5-Fluorouracil and polyphenol EGCG exerts suppressive effects on oral cancer cells exposed to radiation*. Archives of oral biology, 2019. **101**: p. 8-12.
 133. De Rossi, S.S., et al., *A phase II clinical trial of a natural formulation containing tea catechins for xerostomia*. Oral Surgery, Oral Medicine, Oral Pathology and Oral Radiology, 2014. **118**(4): p. 447-454.e3.
 134. Choi, J.-S., et al., *Radioprotective Effect of Epigallocatechin-3-Gallate on Salivary Gland Dysfunction After Radioiodine Ablation in a Murine Model*. Clinical and experimental otorhinolaryngology, 2016. **9**(3): p. 244-251.
 135. Aneja, R., et al., *Epigallocatechin, a green tea polyphenol, attenuates myocardial ischemia reperfusion injury in rats*. Molecular medicine (Cambridge, Mass.), 2004. **10**(1-6): p. 55-62.
 136. Little, J., *Principal cellular and tissue effects of radiation*. Holland-Frei cancer medicine, 2003.
 137. Limesand, K.H., K.L. Schwertfeger, and S.M. Anderson, *MDM2 is required for suppression of apoptosis by activated Akt1 in salivary acinar cells*. Molecular and cellular biology, 2006. **26**(23): p. 8840-8856.
 138. Avila, J.L., et al., *Radiation-Induced Salivary Gland Dysfunction Results From p53-Dependent Apoptosis*. International Journal of Radiation Oncology*Biophysics, 2009. **73**(2): p. 523-529.
 139. Levine, A.J., *p53, the cellular gatekeeper for growth and division*. cell, 1997. **88**(3): p. 323-331.
 140. Kobayashi, M. and M. Yamamoto, *Molecular mechanisms activating the Nrf2-Keap1 pathway of antioxidant gene regulation*. Antioxid Redox Signal, 2005. **7**(3-4): p. 385-94.
 141. Borrego-Soto, G., R. Ortiz-López, and A. Rojas-Martínez, *Ionizing radiation-induced DNA injury and damage detection in patients with breast cancer*. Genetics and molecular biology, 2015. **38**(4): p. 420-432.
 142. Dube, A., J.A. Nicolazzo, and I. Larson, *Chitosan nanoparticles enhance the intestinal absorption of the green tea catechins (+)-catechin and (-)-epigallocatechin gallate*. European Journal of Pharmaceutical Sciences, 2010. **41**(2): p. 219-225.
 143. Granja, A., et al., *EGCG intestinal absorption and oral bioavailability enhancement using folic acid-functionalized nanostructured lipid carriers*. Heliyon, 2019. **5**(7): p. e02020.



จุฬาลงกรณ์มหาวิทยาลัย
CHULALONGKORN UNIVERSITY

VITA

NAME Erni Sulistiyani

DATE OF BIRTH 12 Februari 1989

PLACE OF BIRTH Bantul, Indonesia

**INSTITUTIONS
ATTENDED** Universitas Gadjah Mada

HOME ADDRESS Bejen Bantul RT 06 No.164 Bantul, Bantul, Bantul,
Daerah Istimewa Yogyakarta 55711 Indonesia

Diana Court 262 Petchburi Road Thanon Phetchaburi
Ratchathewi Bangkok Thailand 10400



จุฬาลงกรณ์มหาวิทยาลัย
CHULALONGKORN UNIVERSITY